AD-A045 116 OKLAHOMA STATE UNIV STILLWATER FLUID POWER RESEARCH --ETC F/G 11/8
THE SURVIVABILITY CHARACTERISTICS OF FLUID POWER COMPONENTS IN --ETC(U)
DEC 76 N00014-75-C-1157

UNCLASSIFIED OSU-FPRC-6N1 NL

1 OF 1
ADA045116

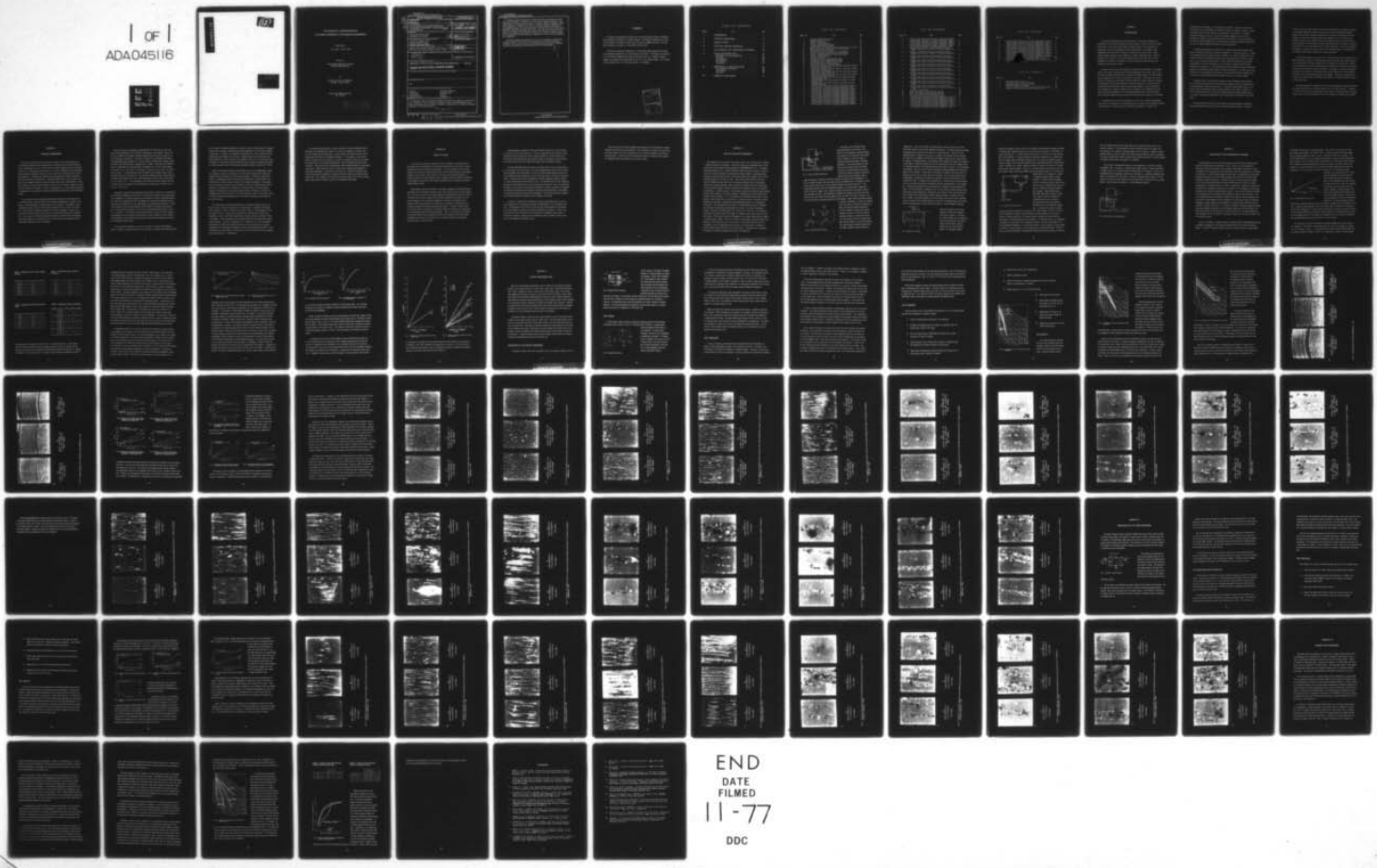

END
DATE FILMED
11-77
DDC

THE SURVIVABILITY CHARACTERISTICS OF

FLUID POWER COMPONENTS IN CONTAMINATED ENVIRONMENTS

Annual Report

1 July 1975 – 30 June 1976

Prepared By

FLUID POWER RESEARCH CENTER
Oklahoma State University

For

OFFICE OF NAVAL RESEARCH
Arlington, Virginia 22217

Contract No. N00014-75-C-1157
NR. 212-232

UNCLASSIFIED

SECURITY CLASSIFICATION OF THIS PAGE *(When Data Entered)*

REPORT DOCUMENTATION PAGE

READ INSTRUCTIONS BEFORE COMPLETING FORM

1. REPORT NUMBER: OSU-FPRC-6N1
2. GOVT ACCESSION NO.
3. RECIPIENT'S CATALOG NUMBER

4. TITLE *(and Subtitle)*: THE SURVIVABILITY CHARACTERISTICS OF FLUID POWER COMPONENTS IN CONTAMINATED ENVIRONMENTS.

5. TYPE OF REPORT & PERIOD COVERED: Annual Report. 1 July 1975 – 30 June 1976.

6. PERFORMING ORG. REPORT NUMBER

7. AUTHOR(s): Fluid Power Research Center, Oklahoma State University

8. CONTRACT OR GRANT NUMBER(s): N00014-75-C-1157

9. PERFORMING ORGANIZATION NAME AND ADDRESS: Fluid Power Research Center, Oklahoma State University, Stillwater, Oklahoma 74074

10. PROGRAM ELEMENT, PROJECT, TASK AREA & WORK UNIT NUMBERS

11. CONTROLLING OFFICE NAME AND ADDRESS: Office of Naval Research, Department of the Navy, 800 North Quincy Street, Arlington, Virginia 22217

12. REPORT DATE: December 1976

13. NUMBER OF PAGES: 84

14. MONITORING AGENCY NAME & ADDRESS *(if different from Controlling Office)*: 89p.

15. SECURITY CLASS. *(of this report)*

15a. DECLASSIFICATION/DOWNGRADING SCHEDULE

16. DISTRIBUTION STATEMENT *(of this Report)*

Reproduction in whole or in part is permitted for any purpose of the [illegible] Government.

APPROVED FOR PUBLIC RELEASE; DISTRIBUTION UNLIMITED

17. DISTRIBUTION STATEMENT *(of the abstract entered in Block 20, if different from Report)*

18. SUPPLEMENTARY NOTES

N/A

19. KEY WORDS *(Continue on reverse side if necessary and identify by block number)*

Hydraulic
Contaminant
Contamination
Contaminant Wear
Hydraulic Components
Wear Mechanisms
Particles
Ferrogram

20. ABSTRACT *(Continue on reverse side if necessary and identify by block number)*

Contaminant wear in fluid power components has long been recognized as a major factor which influences the life and reliability of hydraulic systems. Ignoring catastrophic type failures, contaminant wear of hydraulic components is characterized by a gradual but persistent degradation in external performance.

→ over

DD FORM 1 JAN 73 1473 EDITION OF 1 NOV 65 IS OBSOLETE

UNCLASSIFIED

SECURITY CLASSIFICATION OF THIS PAGE *(When Data Entered)*

A hydraulic system is comprised of a series of individual components and, like a chain, the survivability of the system is no better than its weakest component. The components of a hydraulic system consist of a relatively complex arrangement of fairly simple mechanisms. Therefore, the solution to improved component mortality lies in an investigation of the most common and critical mechanisms and the influence of particulate contaminant upon their performance. Thus, the primary goal of this overall effort is to investigate the improvement in service life which can be expected by the removal of the particulate contamination entrained in the fluid of a hydraulic system. This is accomplished by actual testing work performed on critical hydraulic component wear mechanisms.

The report presents the background from which the investigation originated and outlines the scope of effort for the overall program and the first year's activities. In addition, the nature and extent of the testing program which has been completed during this reporting period is presented along with the results obtained.

FOREWORD

This report was prepared by the staff of the Fluid Power Research Center at Oklahoma State University of Agriculture and Applied Sciences. The study was initiated by the Office of Naval Research at Arlington, Virginia, under Contract No. N00014-75-C-1157. The time period covered by this report is 1 July 1975 to 30 June 1976.

This study was effectively monitored by Lt. Dick Miller, whose guidance and participation contributed significantly to the overall success of the effort. The program was conducted at the Fluid Power Research Center under the direction of Mr. R. K. Tessmann, Program Manager, with guidance and consultation from Dr. E. C. Fitch, Center Director. Mr. Tessmann was ably assisted by Mr. D. E. Kitzmiller and Mr. J. M. Howsden.

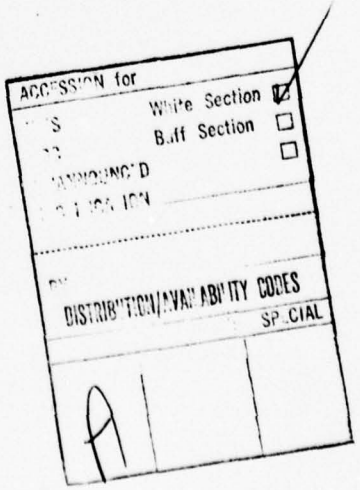

TABLE OF CONTENTS

LIST OF FIGURES

LIST OF FIGURES

LIST OF FIGURES

LIST OF TABLES

CHAPTER I

INTRODUCTION

It has long been recognized that contaminant wear in fluid power components is a primary factor in the life and reliability of hydraulic systems. Except in the case of castastrophic failure (such as valve spool stickage), contaminant wear in such components is characterized by a gradual degradation in external performance. For example, a fixed-displacement pump will exhibit a gradual but persistent loss of output flow at a given rotational speed and pressure when subjected to a critical contamination level. Since the purpose of such a pump is to supply the hydraulic system with a given flow, the flow degradation is a measure of the amount of service life which has been used due to the contaminant wear that has occurred.

In general, there are two critical aspects in determining the acceptability of a hydraulic system. One factor is concerned with the initial performance of the system. That is, will the system accomplish the desired task in a stable, controllable manner? The second consideration is associated with the life and reliability of the system. Performance, life, and reliability of all systems are inter-related, in that the ability of a system to perform the desired tasks adequately is the ultimate measure of its life and reliability. It is convenient when considering contaminant wear to lump these parameters together in terms of survivability. The survivability of a hydraulic component can be thought of as the probability that component performance degradation due to contaminant-accelerated wear will be acceptable after a prescribed operating period at specified operating conditions expressed as a percentage.

A hydraulic system is normally comprised of a series or set of individual components. Like a chain, the survivability of a fluid power system is no better than its weakest component. The major problem in determining the survivability characteristics of a system is the

identification of this weakest or most failure-prone component. However, even when the identification can be accomplished, the suspected component is usually so complex in design and operation that an orderly approach to improvement is very difficult. Fortunately, hydraulic components consist of a relatively complicated arrangement of fairly simple mechanisms. Therefore, the most obvious solution to the problem of improved component mortality lies in the investigation of the most common and critical mechanisms and the influence of the various operational parameters upon their performance.

In attempting to increase the service life of a hydraulic system without specific knowledge of the wear modes which are dominant, designers will – more often than not – choose a more efficient filter than would normally be utilized. In so doing, he assumes that, if the removal of some of the contaminant present in the circulating fluid of the system is good, then if more is removed it must be better. Since he does not understand the survivability characteristics of the system components, he has no way of relating the better filtration provided to an increase in life. The program reported here is designed to provide information relative to the survivability characteristics of hydraulic components. The primary goal of the overall effort is to investigate the improvement in service life which can be expected by the removal of the particulate contaminants entrained in the fluid of a hydraulic system.

Through the work of the Fluid Power Research Center at Oklahoma State University [1], it has been shown that hydraulic components are sensitive to both the particle size and the concentration of particulate contaminant. In reducing the contamination level of a hydraulic system through filtration, both of these parameters will be altered. Therefore, in order to assess the reduction in wear which is associated with lower contamination levels, it is necessary to include both contaminant size and concentration as parameters in the investigation.

This report covers the first year of effort under the program designed to explore the relationships between component life and the contamination level to which it is exposed.

In order to include as many aspects of contaminant-accelerated wear as possible in the study, it was deemed impractical to conduct lengthy tests on relatively expensive components. Instead, two of the basic mechanisms associated with fluid power components which were available at the Fluid Power Research Center were adapted for use in this effort. One mechanism consists of one rotating surface and one stationary surface. This arrangement closely simulates the action between the wear plates and the sides of the gears in a hydraulic gear pump or the valve plate/cylinder block in a piston type pump. The second mechanism was designed to duplicate the relative motion of the spool-bore design of a hydraulic valve or the piston-cylinder block arrangement in a piston type pump.

A major problem which has stymied work in contaminant wear of fluid components has been the inability to explore the processes taking place in the wear region. With the advent of the Ferrographic Oil Analysis Technique [2], this problem has been overcome. While it is still not possible to view the contaminant wear process directly, a study of the wear debris which result can provide the necessary information. Ferrography is a relatively new technology which, at the initiation of this program, had not been widely used to study hydraulic component wear or contaminant-accelerated wear processes. Therefore, it was necessary to include in this study an effort to determine the capability of Ferrographic analysis in regard to contaminant wear.

This report presents the background from which this investigation originated and outlines the scope of effort both for the overall program and the first year's activities. In addition, the nature and extent of the testing program which has been completed during the reporting period as well as the results obtained from the tests conducted are presented and discussed.

CHAPTER II

TECHNICAL BACKGROUND

The term *survivability* as used in this report is meant to imply that characteristic of a fluid power component which is associated with its inherent ability to resist contaminant attack. Abrasive wear is one of the most critical and costly problems faced by an industrial economy [3]. This statement was written by E. F. Finken in 1969; and, while considerable research has been conducted in the area since that time, totally adequate solutions have not been advanced. In a classical sense, abrasive wear encompasses three different phenomena – two-body, three-body, and erosive wear. Two-body abrasion refers to the case where there are only two surfaces involved and micro-cutting takes place due to surface asperities. Three-body abrasion (now more commonly called *contaminant wear*) is meant to imply the presence of a third member in the process – namely, a defiling particle. The erosive wear phenomenon is characterized by the collision of free-moving contaminant particles with a critical component surface.

In a fluid power system, contaminants will become entrained in the circulating fluid from several sources. Since the source of such entrained contamination is irrelevant in this project, no further discussion of possible sources will be presented. The presence of these contaminant particles will result in what has been termed *three-body abrasion* and erosive wear. The amount of contaminant entrained in the fluid is presented in terms of a contamination level, which usually consists of both a particle size distribution and a concentration. Thus, in order to realistically describe the abrasive wear which occurs in fluid power components subjected to a contaminated fluid, both the particle size distribution and the contaminant concentration must be considered.

Many of the previous investigators [4,5,6,7,8,9,10,11,12] who chose to study the abrasive wear phenomenon did not consider enough aspects of the problem. That is, the tests were conducted using greatly simplified mechanisms controlling only particle size or only contaminant concentration, or they were conducted in an unlubricated environment. These deficiencies were spotlighted at a friction and wear interdisciplinary workshop hosted by NASA, Lewis Research Center, Cleveland, Ohio, in 1968. In the report from Working Group II, Unlubricated and Lubricated Wear, transmitted by D. G. Flom, Group Leader, it was stated, *"One of the biggest interdisciplinary deficiencies in wear studies is incomplete characterization."* A classic example of this is illustrated by the different ways in which researchers view the same experiment. The lubrication investigator knows in great detail the composite and structure of his oil; but, when asked about the metal used, he may answer *"It's some kind of steel."* The metallurgist, on the other hand, knows precisely what kind of metal or alloy he is using; but, when asked about the lubricant, he is liable to say *"It came out of this bottle."*

Although the incomplete characterization has always been a problem in an interdisciplinary area such as tribology, the real problem is that the more "classical" wear research could not be translated to a complex component nor interpreted in terms of performance degradation. When it is realized that the life and reliability of a fluid power component are only meaningful when evaluated in terms of performance, the dilemma becomes obvious. In light of this situation, the Fluid Power Research Center (FPRC) at Oklahoma State University took an entirely different approach to the study of contaminant-accelerated wear in fluid power components. In this work, which has spanned some 14 years, the entire component was subjected to various controlled contamination levels while operated at fixed conditions. The performance of the component was monitored to determine the degradation caused by each contaminant exposure [15].

The test procedure developed as a result of the work at the Fluid Power Research Center was called a contaminant sensitivity test and sought to appraise contaminant-accelerated

wear in terms of component performance. Obviously, since a sufficient amount of contaminant was used to produce a measurable performance degradation, the test must be classified as destructive. In addition, the component was operated at the "rated" conditions, which dictated large power demands in some cases. However, based upon a contaminant wear model advanced as a result of this work and presented in Ref. [1] for a fluid power pump, the results of a contaminant sensitivity test can be used to estimate contaminant service life of a given component under the contaminant protection provided by a given filter [14,15].

While this contaminant sensitivity work overcame many of the disadvantages of earlier work (inability to relate to performance), it did not provide insight into the actual wear processes affecting survivability of fluid power components. The legacy of these efforts, however, is overwhelming evidence that even low concentrations of small particles in the system fluid can seriously reduce the service life of hydraulic components. Unfortunately, all of the contaminant sensitivity work has been done on entire components using external performance measurements as an indication of contaminant wear. No effort has been expended in determining the actual wear processes involved. Therefore, it is difficult to extrapolate the results to very high or very low contamination levels. Only through a study of the active contaminant-accelerated wear in fluid power components can the validity of this work be shown.

The major problem which has stymied efforts in contaminant wear has been the inability to explore the action taking place in the wear region. Fortunately, there appears to be a bright ray of hope in respect to this problem. While it is still impossible to view the contaminant wear processes directly because of the enclosed nature of fluid power components, a study of the debris generated during the wear process can provide a wealth of information. A new technology area has evolved which now makes wear debris analysis a viable approach. This area is Ferrography [16]. Through the use of this technological breakthrough, the debris which originates because of the wear process can be evaluated independent of the contaminant introduced to create the contaminated environment. Such an analysis has not been possible in the past, since the wear particles could not be separated from the wear catalyst – contamination.

In an actual fluid power system, a filter is provided to remove contaminant which is entrained in the circulating fluid. Since at this time it is impossible to procure a filter which will remove all such contaminant, a system designer must select the filter that will provide what he considers to be adequate protection. If, in operation, the life and reliability of the system are not sufficient, it is common to replace the filter with one which will remove more of the entrained contamination. Then, the question becomes an economical one. The cost of the new filtering system must be weighed against the improvement in system life. While contaminant wear is a major cause of performance degradation in fluid power components, it is obviously not the only one. Therefore, this program was initiated to evaluate the magnitude of increase in life which results from reduced contamination levels. The remainder of this report will discuss the scope of effort for the overall program and present the results of the first of the proposed three phases.

CHAPTER III

SCOPE OF EFFORT

In a fluid power component, contaminant wear is influenced by several parameters. The particle size and concentration of the entrained contaminant will act jointly to cause destruction of critical surfaces and fluid passages. The type of material used for critical surfaces will influence the contaminant wear rate as will the loading which prevails between surfaces in relative motion. While there are many more such influential parameters, it should be obvious from those pointed out that a program intended to evaluate improvement in survivability characteristics of fluid power components must be separated into carefully planned phases of effort.

This program consists of three phases. Each phase is designed to provide quantitative information that has immediate value and can be used to guide and focus further investigations. The major objective of the overall program is the development of data and information which can be used to evaluate and/or accurately estimate the survivability of fluid power components. From a technical standpoint, it would be a horrendous task to approach a fluid power component as a black box, not knowing or caring what occurs internally during the contaminant-accelerated wear process. In order to produce useful survival data with such an approach, it would be necessary to evaluate every configuration of every component under all operating conditions. Thus, the first phase of this program was directed toward the basic mechanisms which are the building blocks of fluid power components and determine the characteristics of the debris produced by contaminant-accelerated wear of such mechanisms.

The second phase is intended to utilize the information derived from the first phase and extend it to the entire component. In this way, useful data can be acquired from the mechanism tests and verified from work on actual components. The third phase of the overall effort would consider the entire hydraulic system to demonstrate that the information derived during the first two phases will correlate with actual system operation.

The basic mechanisms which were used in the testing effort of the first phase consist of a rotary device and a linear device. The rotary mechanism was made up of one rotating and one stationary disc with hydraulic fluid forced to flow radially between the two discs. This arrangement closely duplicates one of the critical wear areas in all types of fluid power pumps. The linear device (so named because of the linear reciprocating motion) consists of a spool moving back and forth through a bore. The arrangement of the linear mechanism simulates the configuration found in piston pumps and many types of valves. By using these mechanisms in tests where the contaminant environment is carefully controlled and measuring the resulting wear debris with Ferrographic and particle counting techniques, it was possible to evaluate the influence of several critical parameters. The actual test procedures followed and the results obtained are delineated in later sections of this report.

In addition to conducting and analyzing the results of contaminant tests on the two basic mechanisms, the first phase also evaluates the characteristic of the Ferrographic technique. The importance of this task lies in the fact that a test contaminant is introduced into the test system to produce the controlled contaminant environment. In theory, this contaminant (AC Fine Test Dust) will not influence the Ferrographic results, since it is non-metallic. However, it was felt that this assumption must be verified in order to have faith in the analysis of the mechanism tests.

The next section of this report discusses the evaluation of the Ferrographic oil analysis technique and presents the results obtained. This is followed by a section which reveals the extent and results of the rotary mechanism work and a section dedicated to the efforts on the linear device. The final part of the report will consist of a summary and will present the conclusions which can be drawn from the work to date.

CHAPTER IV

TEST DATA ANALYSIS TECHNIQUES

Test samples taken, as outlined in the previous section, were analyzed by two methods – particle counting and Ferrography. The particle counts were accomplished using a HIAC Particle Size Analyzer, Model PC-320 calibrated per ANSI/B93.28-1973 [17]. Ferrographic analysis was carried out on a Foxboro/Trans-Sonic Duplex Ferrograph Analyzer in conjunction with a Foxboro/Trans-Sonic Ferroscope and Ferrogram Reader. Contamination level analysis by particle counting has been a fluid power industry-wide accepted method of contamination analysis for a number of years. A late model particle counter (such as the Center's PC-320) has proven itself to be an accurate and valuable tool in contamination analysis when properly calibrated. Since this method of analysis has been so widely used in the fluid power industry, a lengthy explanation of its operation would, in all likelihood, be superfluous. In general, however, it may quickly be stated that an optical particle counter moves by some method, in this case air pressure, a predetermined volume of sample fluid through a counting chamber. It is in this chamber, as the particles pass through, that they interrupt a beam of light from a light source to a photo-cell pickup. The amount of light blocked by the particle is measured and transformed electronically into a corresponding particle size. The instrument sums the number of particles greater than each pre-selected size; and, when the sample has passed through the counter, the results are presented in number of particles per millilitre greater than the given size. (See Fig. 1 for a schematic.) The particle count data as used in this report are averages of three counts made from each fluid sample. Unlike particle counting, Ferrography is not a widely used method of analysis in the fluid power industry. This is not to imply that Ferrographic results are viewed with suspicion by the industry, for such is not the case. It rather stems from the fact that Ferrography is not in widespread use only because of the small number of machines in existence (approximately 25 at the time of this writing). In accordance with its newness, the authors will devote considerably more space to its explanation.

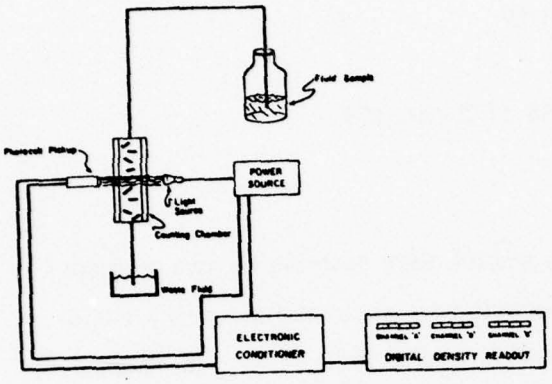

Fig. 1. Schematic of Optical Particle Counter.

The basis of the immediate success (and high promise for the future) is the ability of the Ferrograph to separate metallic wear debris from the particulate contaminant which is added to a system in order to accelerate the wearing process in laboratory evaluations. In the past, analysis by microscopy of wear debris has been frustrating at best and a complete failure at its worst. The need to remove extraneous contaminant particles from a filter membrane used to collect wear debris is evident from the first moment of viewing at high magnification. In order to allow the study of the wear debris from an accelerated test, it is necessary to separate the metallic wear debris from the (usually crystalline) contaminant particles. In the Ferrographic technique, this is accomplished by passing an oil sample across a glass slide which is fixed in a magnetic field. Metallic particles are captured by the magnetic field as they pass down the slide. The preparation is completed by passing a fixer across the slide (after the entire oil sample has been passed) to wash the slide, now called a Ferrogram, free of oil and to affix the captured particles to the Ferrogram. Figure 2 shows the steps necessary to prepare a Ferrogram. In truth, the magnetic field is not alone in retaining the particles, as there are three basic capture mechanisms. The first is simply a "settling out" process, whereby the particles enter a flow field at insufficient velocity to sustain their motion. The fluid velocity across the Ferrogram has been carefully chosen to minimize this effect. The second capture mechanism which enters into debris collection, unless controlled, is

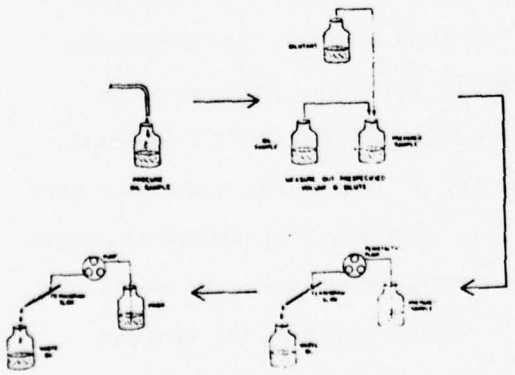

Fig. 2. Ferrogram Preparation Procedure.

"logjamming." As the name implies, this phenomenon is simply the capture of moving particles by stationary ones through mechanical interference. If sufficient particles are present, these agglomerations may grow very large (on a microscopic scale). The last and most significant capture mechanism is, of course, the magnetic field induced along the substrate. The lines of flux throughout the field cross the Ferrogram laterally and are usually traced by "strands" of captured particles. Since magnetic field strength varies sharply with distance, a small angle of inclination between the axis of the slide and the axis of the magnet results in a significant gradient in the magnetic field along the length of the slide. This accomplishes two purposes. The first is that it allows the particles to deposit themselves along the entire length of the Ferrogram. If there were no inclination, the magnetic field would reach full strength very near to the oil entry end of the Ferrogram, and many more particles would be deposited in a relatively short distance and, therefore, in such a high density as to be unsuitable for study. Incidental to this "spreading out" of particles but of extreme benefit is the fact that now the particles are positioned along the slide according to their magnetic size. Ferrous particles range in size from fractions of a micrometre to 50 micrometres or larger. The larger particles are deposited first on the slide while the smaller particles travel some distance before precipitating. Although the vast majority of wear debris particles are ferrous material, other metals exhibit sufficient magnetic properties to deposit along the slide. However, since these properties are so much weaker than those of ferrous materials, a brass or aluminum (for example) particle of a given size will usually deposit much farther down the Ferrogram than an equal sized ferrous particle. Figure 3 depicts a Ferrogram.

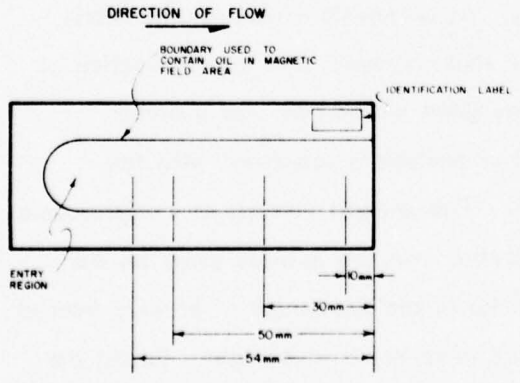

Fig. 3. Illustration of a Ferrogram.

After the Ferrogram slide has been prepared, there are two methods of study used to analyze it. The first is a strictly objective one of measuring the volume of debris on the slide by taking an optical density reading through the use of the Ferrogram Reader. The Ferrogram Reader

operates by impinging a beam of light on the Ferrogram and electronically reading the amount of reflected light. Metallic particles, even in the very small sizes found on a Ferrogram, are opaque and reflective. It is these particles which account for the bulk of the light reflected back to the photocell. In contrast, particles of some given compound (even a metallic one) while still opaque reflect considerably less light back to the source, and crystalline particles transmit or refract most of the light received by them, again reflecting back a relatively small amount. Therefore, the "density" reading is primarily a function of the amount of metallic debris present on the Ferrogram. Figure 4 is a schematic tracing the operation of the Ferrogram Reader. While the Ferrogram Reader will give quantitative results as to the amount of metallic debris on a Ferrogram, it is unable to distinguish between different metallic materials. In order to acquire knowledge not only of the total amount of debris on the slide but also of the gross particle size distribution, a number of readings are taken on the Ferrogram. These readings (termed DEN, D54, D50, D30, and D10) are taken in the region of the entry deposit, 54 millimetres from the exit end (that is opposite the entry end), 50 millimetres, 30 millimetres, and 10 millimetres, respectively. As previously explained, the debris magnetic particle size is related to its position on the slide; however, it is also a function of particle composition; therefore, density readings at any given position are not a prime indicator of actual particle size. The second method of analysis is concerned with the identification of individual particles on the Ferrogram. This analysis consists of a microscopic examination of the Ferrogram by an experienced operator. His job is made easier by the special Bichromatic Microscope. In many cases, particles in the size ranges of primary interest are difficult to identify based only on their appearance in reflected white light. To aid the analyst in particle identification, the Bichromatic Microscope allows the operator to shine red

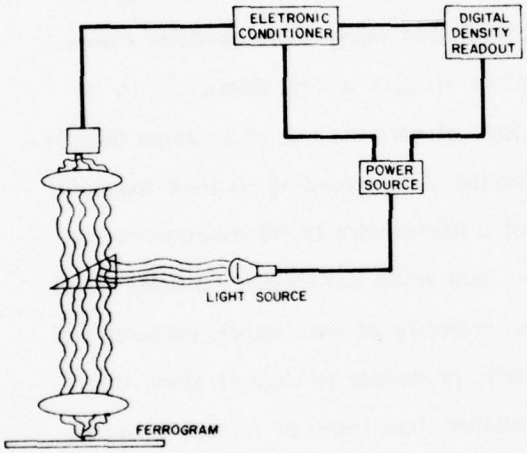

Fig. 4. Schematic of Ferrogram Reader.

from the reflected light source and green light from the transmitted light source on the particle in question. As stated previously, metallic compound particles are opaque, with low reflectively, and crystals are translucent, again with low reflectivity. Therefore, particles appearing bright red only are metallic, and particles appearing distinctly green are crystalline. This feature, coupled with operator experience, allows rapid identification of literally hundreds of different materials which may appear on a Ferrogram.

The last piece of Ferrographic equipment to be discussed here is the Direct Reading Ferrograph or D.R. This again is an optical density reader; however, it allows measurement of metallic debris in an oil sample without the preparation of a Ferrogram. The D.R. unit accomplishes this by magnetically collecting the wear debris in a small glass precipitator tube, where it is illuminated by a light source. Unlike the Ferrogram Reader, however, the D.R. measures the amount of light blocked by the particles present and converts this to an optical density. Figure 5 shows the operation of a Direct Reading Ferrograph.

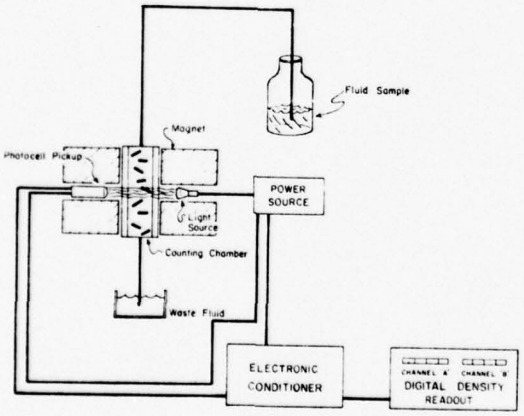

Fig. 5. Schematic of Direct Reading Ferrograph.

CHAPTER V

EVALUATION OF THE FERROGRAPHIC TECHNIQUE

This project was one of the two initial programs at the Fluid Power Research Center utilizing the Ferrograph for interpretation of data. As such, it has been necessary to thoroughly evaluate the technique in order to attain a high degree of proficiency in both the operation of the equipment and the interpretation of the data supplied by the Ferrograph. In these areas, it is felt that great progress has been made in understanding the Ferrographic technique with regard to its use and abuse, strengths, and limitations for evaluating wear situations in hydraulic applications. Although a number of articles regarding Ferrography [2, 18, 19, 20] have been published, the Center believes itself to be the first to utilize Ferrography on a large-scale basis as a *fluid power* analysis tool. Therefore, this project was initiated with no preconceived concepts of the suitability of the Ferrograph for this purpose but rather with a scientific attitude toward its results. It was felt that initially the operation of the Ferrograph must be dictated by the guidelines set forth by the manufacturer. Later, as the project staff became increasingly familiar with its operation, judicial investigation into the validity of those guidelines could be considered. As the programs using the Ferrograph progressed, it became apparent that investigations into several areas of operation would be beneficial. In general, there were: (1) variations in readings, including the agreement between the particle densities as obtained from the Ferrogram Reader and the Direct Reading Ferrograph; (2) the effect of the presence of AC Fine Test Dust in the oil samples analyzed by the Ferrograph; and, (3) the variations in readings or results of any sort from multiple "runs" of the same oil sample.

Early in the program, a sufficient number of samples had been Ferrographically analyzed to enable an investigation into the agreement between the D.R. unit and the Ferrogram Reader. As noted in the previous section, the D.R. unit should register an optical density

of 200 when the light path is completely blocked. Under similar circumstances, the Ferrogram Reader should register its full scale or 100. The density readings from both methods were then plotted against one another in order to graphically depict this relationship. The DRI and DRE (These refer to the manufacturer's designation of large and small, respectively.) were compared to all the Ferrogram Reader densities (that is, the DEN, D54, D50, D30, and D10). Since the full-scale relationship was one-to-two, a slope of .50 should indicate exact correlation. As may be noted from Fig. 6, the DRI and D54 readings give very nearly the desired result. In fact, the slope of the line in Fig. 6 is .54. At a later date, another correlation curve was obtained (from a study specifically designed to provide these data) utilizing fewer data points but taking the mean of three measurements for each density. The slope of this curve is .58. The correlation is fairly good on this curve over the entire range of readings. During this study, it was noted that the particle density reading at the 54 millimetre (D54) position on the slide was the most responsive to the type of tests being carried out. The density readings at 50 and 30 millimetres (D50 and D30) were found to be "good" readings but were less sensitive to the type of wearing situations induced as part of this study, while the density at 10 millimetres seemed totally unresponsive in a great number of cases with its variations being almost random. The entry region (DEN) should have been a reliable indicator of the larger particles; however, the DEN readings showed an inconsistency most probably due to the common occurrence of debris particles being piled one atop the other in this entry region.

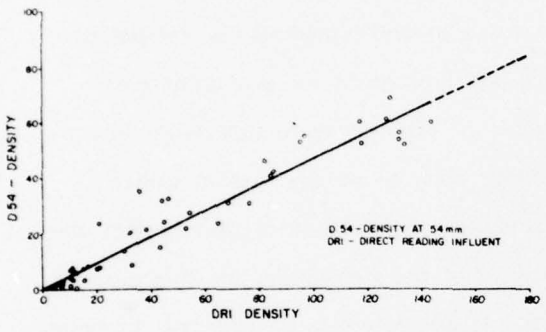

Fig. 6. Ferrogram Density (D54) versus DRI.

At a later date, a study of the variations of multiple readings from the same sample was undertaken. The results for three readings taken for each of four samples run through the D.R. are shown in Table 1. The same type of test was performed with Ferrograms, and the results are shown in Tables 2, 3, and 4. An examination of Tables 1 through 4 leaves

TABLE 1. Repeatability Analysis of Direct Reading Ferrograph.

SAMPLE	DRI	$\bar{X}_{DRI}$	S_{DRI}	$(S/\bar{X})_{DRI}$	DRE	$\bar{X}_{DRE}$	S_{DRE}	$(S/\bar{X})_{DRE}$
1	18.7	19.9	1.85	.09	3.9	5.7	1.59	.28
	18.9				6.3			
	22.0				6.9			
2	35.8	42.0	6.36	.15	16.6	15.4	1.11	.07
	41.6				14.4			
	48.5				15.3			
3	48.0	63.3	13.33	.21	15.3	19.3	3.52	.18
	69.8				20.7			
	72.2				21.9			
4	58.5	76.9	16.30	.21	25.5	27.4	1.85	.07
	89.5				29.2			
	82.4				27.4			

TABLE 2. Repeatability Analysis of DEN and D54 Results.

SAMPLE	DEN	$\bar{X}_{DEN}$	S_{DEN}	$(S/\bar{X})_{DEN}$	D54	$\bar{X}_{D54}$	S_{D54}	$(S/\bar{X})_{D54}$
1	25.8	20.5	5.80	.28	13.1	13.8	.65	.05
	20.8				13.8			
	15.0				14.4			
2	33.1	35.7	2.6	.07	21.1	22.0	2.61	.12
	36.8				19.9			
	38.3				24.9			
3	67.2	54.9	10.65	.19	42.8	38.6	3.81	.10
	48.9				37.5			
	48.6				35.4			
4	74.0	69.8	6.79	.10	40.8	43.4	2.31	.05
	62.0				44.4			
	73.5				45.1			

TABLE 3. Repeatability Analysis of D50 and D30 Results.

SAMPLE	D50	$\bar{X}_{D50}$	S_{D50}	$(S/\bar{X})_{D50}$	D30	$\bar{X}_{D30}$	S_{D30}	$(S/\bar{X})_{D30}$
1	12.1	11.5	.85	.07	1.8	4.0	3.12	.79
	10.5				2.8			
	11.8				7.5			
2	17.3	19.2	1.67	.09	0.0	5.4	4.74	.88
	20.2				7.3			
	20.2				8.9			
3	41.0	34.8	5.53	.16	19.8	18.3	1.67	.09
	33.2				18.6			
	30.3				16.5			
4	37.2	34.9	4.07	.12	24.0	20.8	4.16	.20
	30.2				16.1			
	37.5				22.3			

TABLE 4. Repeatability Analysis of D10 Results.

SAMPLE	D10	$\bar{X}_{D10}$	S_{D10}	$(S/\bar{X})_{D10}$
1	5.3	4.6	.59	.13
	4.2			
	4.4			
2	10.8	16.2	5.05	.31
	17.0			
	20.8			
3	13.2	16.1	5.43	.34
	22.4			
	12.9			
4	16.3	13.1	2.76	.21
	11.9			
	11.2			

little doubt as to the variation of results *possible* in Ferrographic analysis. In these tables, the three readings are given as well as the average reading (e.g., $\bar{X}_{DRI}$), the variance of the readings (e.g., S_{DRI}), and the normalized variance (variance divided by the average, e.g. $(S/\bar{X})_{DRI}$). From Table 1, it may be seen that, in the range of values recorded, approximately the same

confidence level may be placed in the DRI and DRE. Table 2 points out the superiority of the D54 reading as a valid Ferrographic result in that the variations are less. Tables 3 and 4 show the D50 reading to be somewhat substandard to the D54, while the D30 and D10 readings indicate very little confidence may be placed in them. The data scatter observed in these evaluations can be assumed to be present in the test results of this mechanism wear study or in the measurement process itself. Care was taken to insure the verification samples were run using the same procedures and under the same conditions as the day-to-day project samples. The density readings at some positions on the Ferrogram exhibit considerable scatter, but it must be noted that the readings at different positions essentially reflect particles of different magnetic sizes, and it is not unreasonable to expect correlation between various tests would be much better for some particle size ranges than others. In illustration, it has been noted that, when analyzing debris from a pump contamination sensitivity test, the DRI, DEN, D54, and D50 readings are much more responsive to performance parameter changes than the DRE, D30, or D10 readings. The Ferrograph user should not expect any one density number to be his prime indicator on every occasion nor should he expect every density reading to be sensitive to changes in his test parameters. It should also be clear that, if certain of these numbers are responsive to some type of test, it may be expected they could be responsive to closely related tests; and, indeed, this result is borne out by the D54 results following equally well the rotary and linear mechanism tests conducted during this study.

In assessing the effect of AC Fine Test Dust present in literally every sample analyzed in this program, it was necessary to acquire samples of oil with known quantities of ferrous particles in the size range of interest. This was accomplished by use of Carbonyl Iron Powder E in known concentrations. The AC Fine Test Dust (ACFTD) in 0-80 micrometre single-cut used for this evaluation was de-ironized during the cutting process. The de-ironization is a normal procedure at the FPRC and removes most of the ferrous material from the dust. As may be seen in Fig. 8, a gravimetric ratio of ACFTD to Fe of 2:1 affects the DRI reading by approximately 10%, essentially independent of mixture concentration." This study is important in view of the fact that literally all the samples analyzed Ferrographically during this study contain ACFTD. The dust has a minimal effect on the visual analysis of the

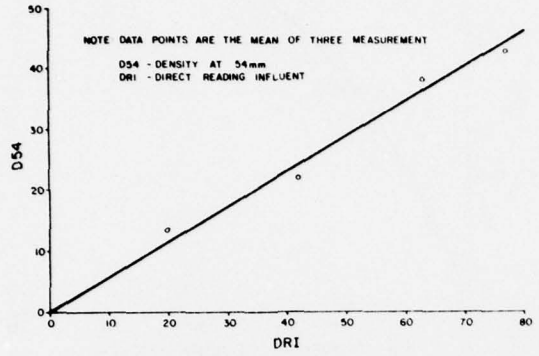

Fig. 7. Results of Study on the Correlation Between Ferrogram Density and D.R. Unit.

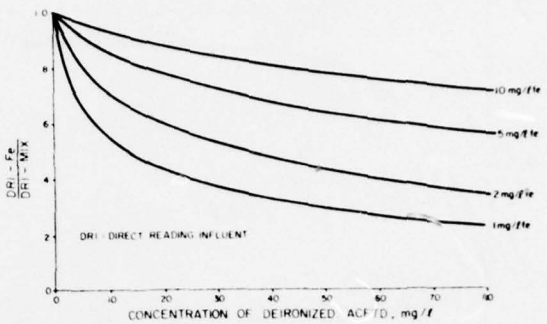

Fig. 8. Results of Study to Determine the Effect of of AC Fine Test Dust.

Ferrograph, since the wear particles are easily identified from the crystalline particles which make up the bulk of the ACFTD. Any crystalline particles present on a Ferrogram are noted; and, as time permits, a more extensive investigation into the appearance of ACFTD may be undertaken. If the presence of these particles represents an obstacle to proper analysis, the oil sample is diluted and a new Ferrogram made. This results in a more efficient analysis, since large amounts of wear debris normally accompany heavy concentrations of ACFTD. The dilution is therefore a double solution, since it allows for easier and probably more accurate analysis. In light of the fact that it was desirable on certain occasions to dilute the oil samples prior to analysis, it was deemed prudent to undertake a study of the effects of this dilution on the density readings taken on both the Direct Reading Ferrograph and the Ferrogram Reader. With no loss of accuracy, this may be termed a study of the relationship of the concentration of particles (in a given sample) to the corresponding density readings. Accordingly, a series of samples of known iron concentration (in clean oil) were prepared and the densities measured by the Direct Reading Ferrograph. The overall results are given in Fig. 9, where the saturation of the instrument is unmistakable. Figure 10 shows the portion of the same curve from zero to an Fe concentration of 50 mg/litre. It appears that the most linear portion of the curve was in the range of 0 to 10 mg/litre. Accordingly, the practice of diluting or concentrating samples (i.e., running a larger sample size) was instituted

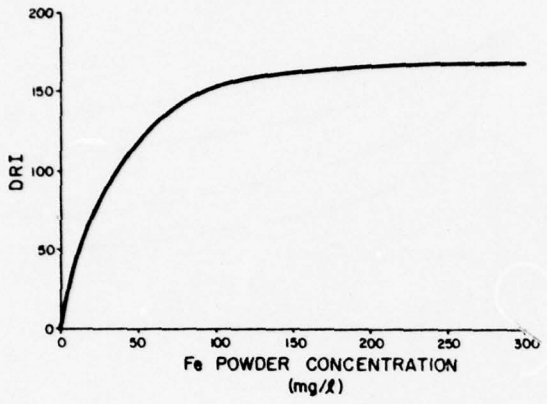

Fig. 9. DRI Density versus Iron Concentration.

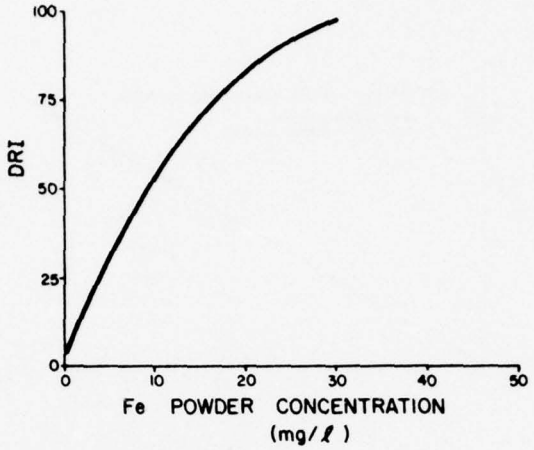

Fig. 10. DRI Density versus Iron Concentration for Low Concentrations.

in an attempt to maintain the density readings in the most linear range. At a later date, the effect of this practice on samples from systems containing both metallic wear debris and ACFTD was investigated.

In order to study the effects of dilution or concentration on the density readings, a series of tests was conducted utilizing multiple readings from the same sample. The results of these tests are shown in Figs. 11 and 12. The D10 and D30 readings have noticeably more scatter than the others. The remaining readings (DRI, DRE, DE, DEN, D54, and D50) give evidence of good linearity in this range of values. This reaffirms the decision to attempt to dilute or concentrate samples as necessary to remain in the linear region of the density instruments utilized.

It is hoped that this section has accomplished its goal of familiarizing the reader not only with the basic theory and operation of the Ferrograph equipment but also with the problem of Ferrographic data interpretation and the operational limits of the equipment. The results, both in terms of the project goals and familiarity with the Ferrographic technique, are sufficient to conclude that the Ferrograph is a unique tool for contaminant wear evaluation. In addition, it seems evident that the Ferrograph is eminently suited to wear studies

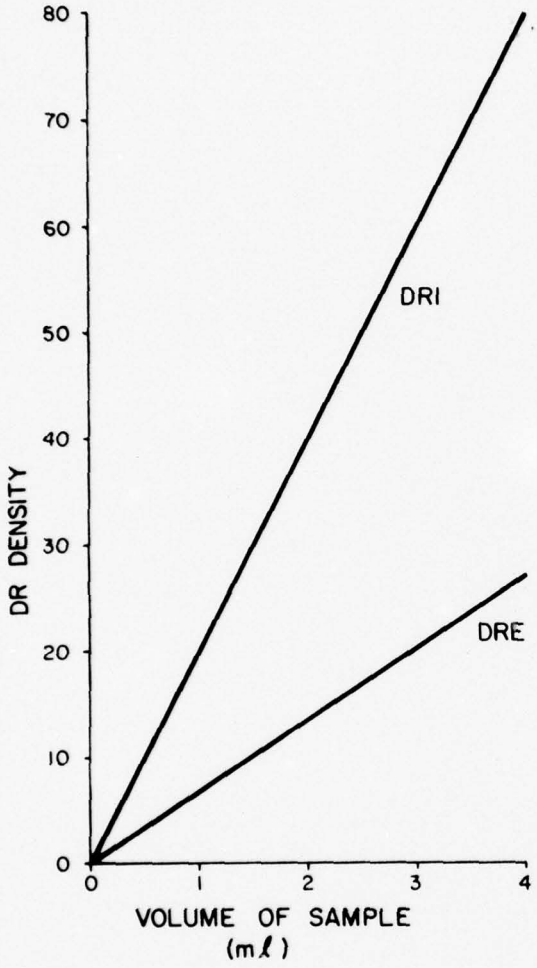

Fig. 11. Linearity of D.R. Density Reading with Various Fluid Volumes.

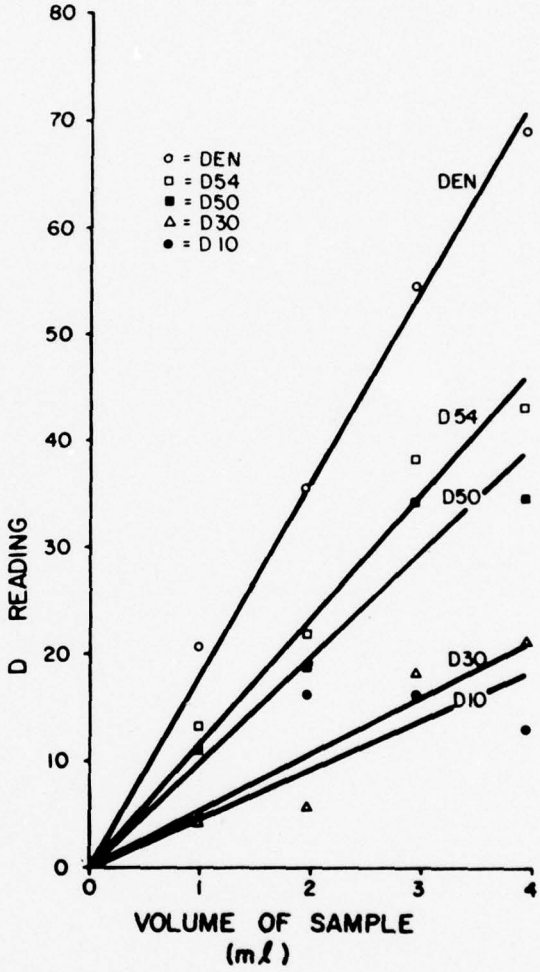

Fig. 12. Linearity of Ferrogram Densities with Various Fluid Volumes.

as conducted in this program and that further research into the operation of the equipment is necessary to more fully understand the valuable data it provides. It is felt that this first year of operation has proved the value of Ferrographic analysis and provided the experience necessary to utilize the Ferrograph even more efficiently.

CHAPTER VI

ROTARY MECHANISM TESTS

One of the most prevalent mechanisms used in the design of fluid power components consists of two surfaces which are in relative rotary motion with a small clearance between them. Such a mechanism is found in most types of high pressure pumps. For example, fluid leakage past the sides of the gears in a gear type pump is controlled by plates (called wear plates) which are pressure loaded against the sides of the gears. Relative clearance between these two surfaces is usually maintained by a critical pressure balance, where hydrostatic and hydrodynamic forces act between the surfaces with pressure forces opposing. Therefore, the actual clearance which would characterize this wear area will depend upon the operating conditions as well as the fluid used. Since the gears are rotating and the wear plates are stationary, the rotary mechanism closely simulates this arrangement.

As another example of where the rotary type mechanism is used in fluid power pumps, consider the valve plate—cylinder block of a piston pump. The reciprocating pistons are contained in the cylinder block, and the valve plate is used to time the piston action with the inlet and outlet ports. Here again, the clearance between the rotating cylinder block surface and the stationary valve plate is controlled by a balance between spring and pressure forces tending to reduce any clearance and hydrostatic/hydrodynamic forces tending to spread the surfaces apart. It should be obvious that the actual clearance between these two surfaces is dictated by operating conditions and fluid characteristics.

DESCRIPTION OF THE ROTARY MECHANISM

A schematic drawing of the rotary mechanism used in this program is shown in Fig. 13.

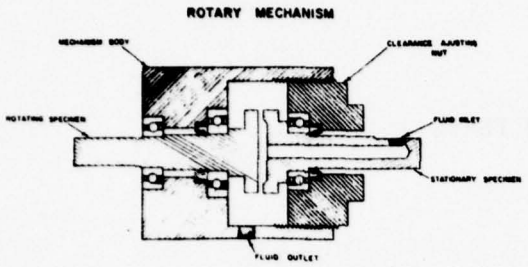

Fig. 13. Schematic of Rotary Mechanism.

As can be seen in this figure, the device consists of a rotating specimen, a stationary specimen, a body, and an adjusting nut. Rotary seals are used to contain the pressurized fluid, and ball bearings carry the thrust load and maintain the relative position of the two specimens. In operation, fluid is forced through the stationary specimen and flows out between the two surfaces. By entraining a known contaminant in the circulating fluid, contaminant wear can be induced in the area where the clearance between the two faces is a minimum. As contaminant wear occurs, the adjusting nut is used to maintain a constant clearance. This was accomplished by maintaining a clearance which results in a constant pressure drop across the mechanism at a fixed flow rate.

TEST SYSTEM

The test system which was used to provide the hydraulic power and the controlled contamination level is shown in Fig. 14. The main pump is driven by a variable speed motor and supplies fluid directly to the mechanism. To permit slight variations in the flow to the mechanism, a bypass valve is provided. A charging pump is included in the circuit, not only to supply fluid to the main pump but also to provide circulation in the reservoir to insure adequate mixing and prevent contaminant settling.

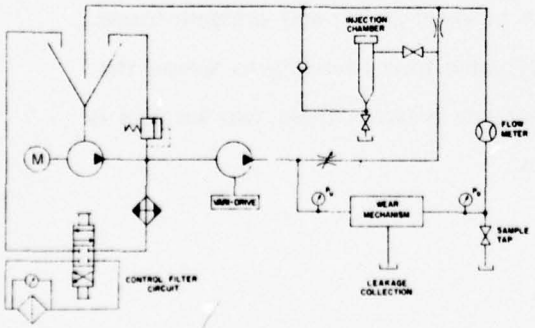

Fig. 14. Schematic of Test System.

In order to inject precise amounts of contaminant into the flowing system once the test conditions are established, an injection subsystem is included. This subsystem consists of an injection chamber and the necessary valving to direct fluid from the bypass line through the injection chamber and into the main return. The fact that the contaminant is injected upstream of the reservoir is important in order to prevent a large slug of contaminated fluid from reaching the test mechanism. By injecting the contaminant into the return line, it mixes with the clean fluid in the reservoir before reaching the mechanism.

To remove the contaminant which was added to the system, control filters are used. The control filter circuit consists of a filter assembly involving a high performance element and a four-way valve which is used to either include the control filter in the circulating system or valve it out. The efficiency of these filters was such that the system could be cleaned in a minimum amount of time.

Before conducting any mechanism tests with this test system, a validation experiment was conducted. Since the objective of the system is to maintain a constant contamination level in the circulating fluid, tests were conducted where the mechanism was replaced by a straight section of tubing. The control filters were removed from the system by means of a four-way valve, and the system fluid was contaminated to a selected level. The system was operated for a period of one hour, and samples were removed periodically. Particle counts on these samples revealed no significant change in the contamination level of the system for this period of time.

TEST CONDITIONS

In order to produce a contamination wear situation which was both possible and realistic, careful consideration was given to the conditions of the test. The decision was made that the tests would be conducted at a constant clearance. However, the exact value of this clearance as well as the magnitude of the flow, pressure drop, temperature, and speed

had to be selected. In addition, the design of the mechanism made it impossible to measure the clearance between the two wear surfaces directly. Therefore, it was necessary to establish an indirect measurement technique for this parameter.

All of the critical parameters associated with the rotary mechanism are inter-related. That is, the flow-pressure drop relationship is dependent upon the clearance selected. In addition, the construction of the mechanism allowed for an increase in clearance when pressure was applied due to a spring effect. However, the mechanism was designed such that the clearance was an adjustable parameter. Therefore, with the mechanism not rotating, it was possible to bring the two surfaces into contact such that almost no flow occurred when subjected to a given pressure drop. Then, the adjusting nut was moved in precise increments, and the flow rate was measured while the constant pressure drop was applied. In this manner, the flow-pressure-clearance relationship for the rotary mechanism was determined experimentally.

In order to acquire additional correlation, a mathematical analysis was made of the rotary mechanism. The analytical expressions which describe the basic relationships for the rotary mechanism under both stationary and rotating conditions were considered. The experimental data obtained from the mechanism were then compared to the analytical results, which revealed close correlation between the two. Therefore, by measuring the flow and pressure drop conditions existing on the mechanism, an accurate estimate of the clearance could be made.

Due to physical limitations, the pressure drop across the rotary mechanism was selected at 400 psid. At pressures above this value, the torque necessary to move the adjusting nut was excessive. The clearance for the battery of tests conducted during this first phase was set at 20 micrometres, which produced a flow rate of about 2.6 GPM using a fluid conforming to Mil-H-5606 at 100°F. Once these parameters were established, it was possible to select the size distribution and concentrations for the contaminant environments. It was felt that the best information would be obtained by using three different particle size ranges – one far below, one slightly above, and one far above the 20 micrometre clearance. Thus, particle size ranges of 0-5, 0-30, and 0-80 micrometres were used. The concentrations selected were

5, 10, 20, 40, and 80 milligrams per litre, with each concentration of all of the particle size ranges being required for the tests. The actual contamination levels used in the mechanism tests are shown graphically in Figs. 15, 16, and 17 for the 0-5, 0-30, and 0-80 particle size ranges, respectively.

Three types of specimen materials were selected based upon the materials commonly used in high-pressure fluid power pumps. In one set of tests, the rotating specimen was fabricated from a 360 free-cutting yellow brass, while the mating stationary part was made of 1020 mild steel. In the other set of tests, the rotating component was machined from 2024-T351 aluminum while again the mating specimen was 1020 mild steel.

TEST PROCEDURE

The test procedure which was developed and followed for all of the tests conducted using the rotary mechanism is outlined as follows:

1. Install the appropriate test specimens in the mechanism.

2. Establish the designated flow rate through the mechanism with the control filters as part of the system.

3. Start the rotating motion (1500 RPM) and operate until a stable temperature of 100° F is reached.

4. Adjust clearance until a pressure drop of 50 psid is measured across the mechanism and operate mechanism for 45 minutes.

5. Repeat Step 4, increasing the pressure differential by 50 psid until a total pressure drop of 400 psid is attained.

6. Remove control filter from circulating loop.

7. Obtain a background sample.

8. Inject 0-5 micrometre contaminant obtained from AC Fine Test Dust stock at a concentration of 5 mg/litre.

9. Obtain samples at 2, 7, 14, 25, and 45 minutes.

10. Filter system for 30 minutes.

11. Repeat Steps 6 through 10 using concentration of 10, 20, 40, and 80 milligrams per litre.

12. Repeat Steps 6 through 11 for particle size ranges of 0-30 and 0-80 micrometres.

13. Repeat entire procedure for various material combinations.

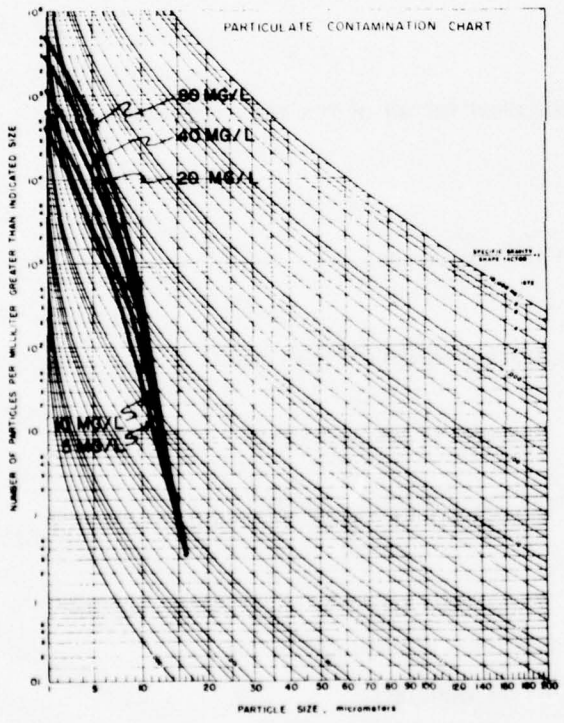

Fig. 15. Contamination Levels for 0-5 Micrometres Particle Size Range.

TEST RESULTS

The samples which were obtained from the rotary mechanism tests were analyzed to determine the total contaminant level and the amount of wear debris. Automatic particle counter

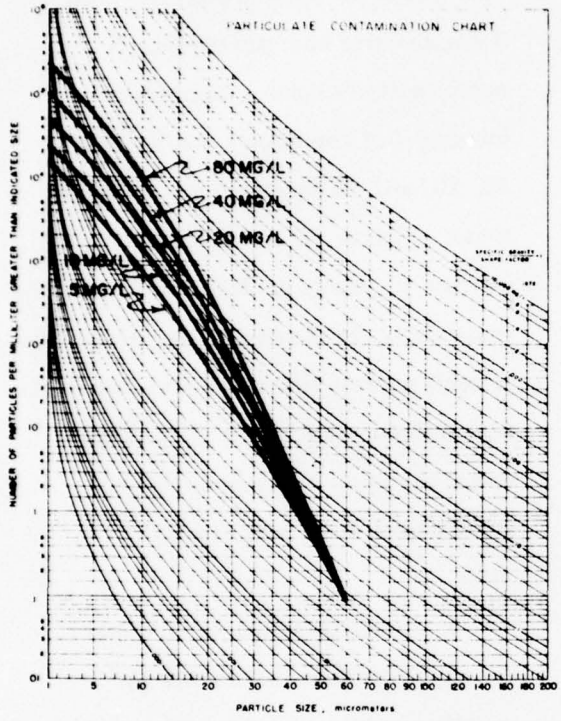

Fig. 16. Contamination Level for 0-30 Micrometre Particle Size Range.

techniques were employed to evaluate the contamination level, and Ferrographic analysis was used to assess the concentration and nature of the wear debris. Since the objective of the tests was to evaluate the amount of wear produced by the various contaminant environments, the results which are presented have been reduced to most clearly meet this objective.

The physical appearance of the test specimens is shown in Figs. 18 and 19 for the brass and aluminum, respectively. Figures 18(a), (b), and (c) reveal the nature of the brass surface after exposure of the 0-5, 0-30, and 0-80 micrometre particle size ranges, respectively; while, Figs. 19(a), (b), and (c) depict the same information associated with the aluminum test specimen. It should be noted from these figures that, in both the case of brass and aluminum, the size of the radial grooves and the magnitude of surface destruction increase with particle size range.

Since, as the test surfaces wear due to the contaminant exposure, the wear debris will become entrained in the fluid, it is possible to assess the magnitude of the wear by measuring the contamination level. Particle counts were performed on the fluid to determine the increase of particles of various sizes that occurred during the tests. Counts were made of the number of particles per millilitre greater than 3, 5, 10, 20, and 30 micrometres. In order to assess the buildup in particle counts, the contamination level due to the injected contaminant (as shown in Figs. 15, 16, and 17) was subtracted from the counts measured at the end of the

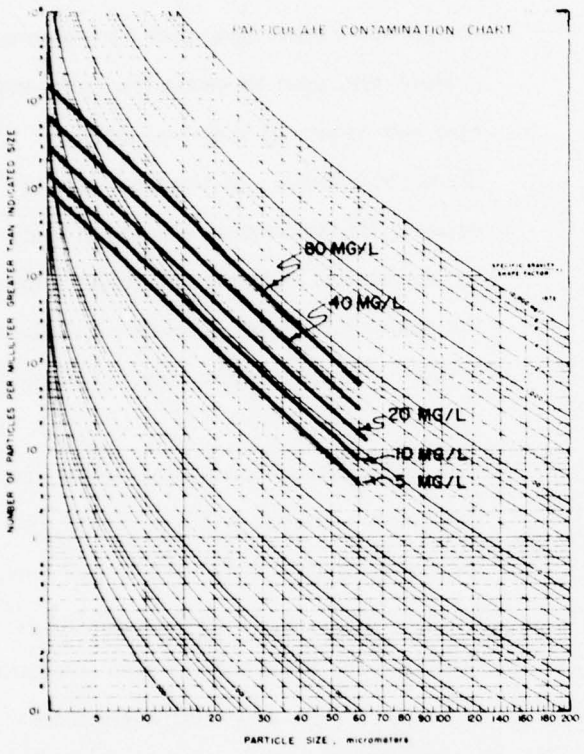

Fig. 17. Contamination Levels for 0-80 Micrometre Size Range.

test for each particle size analyzed. The counts per millilitre greater than 3 micrometres and greater than 5 micrometres revealed a significant increase, but the counts greater than 10, 20, and 30 indicated no significant trend. Figures 20 and 21 illustrate the increase in counts at 3 and 5 micrometres, respectively, for brass-on-steel combinations at each particle size range and concentration utilized; while, Figs. 22 and 23 reveal the same information for the aluminum-on-steel tests.

It should be noted from these figures that, while the increase in particle counts in the brass/steel tests was large at the lower concentrations, it tended to level out at the higher concentrations. However, the shape of the curves obtained from the results of the aluminum/steel investigation reveal an entirely different characteristic. In this case, the magnitude of contaminant buildup was fairly constant at the lower concentrations and was much larger at the 80 milligrams per litre concentration. In both cases, the particle increase with the 0-80 micrometre particle size range was significantly greater at all concentrations than that for the smaller size ranges used.

From the Ferrographic analysis, an interesting fact was revealed. Previous work in contaminant sensitivity indicated that, when contaminant is exposed to a wear area on a multi-pass basis as was done in these tests, the amount of wear would be large initially but would decrease with time. This phenomenon is associated with the destruction of the

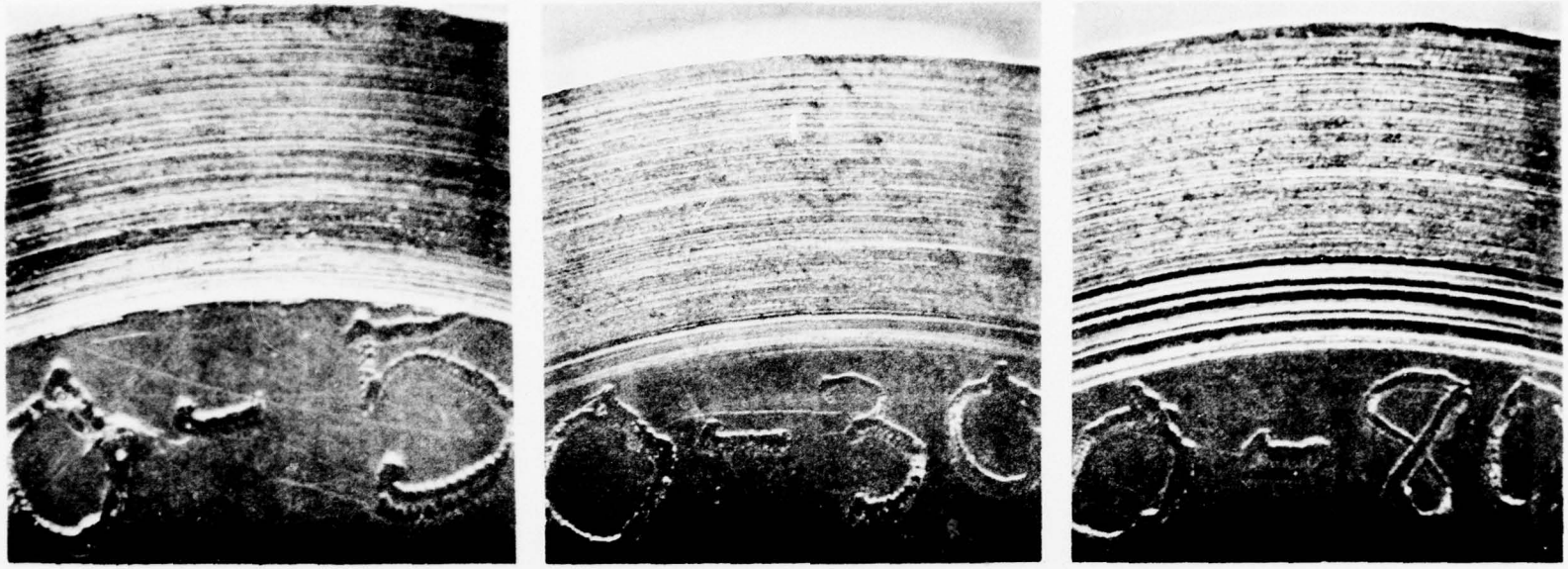

(a)
AFTER EXPOSURE TO
0-5 μM PARTICLE
SIZE RANGE

(b)
AFTER EXPOSURE TO
0-30 μM PARTICLE
SIZE RANGE

(c)
AFTER EXPOSURE TO
0-80 μM PARTICLE
SIZE RANGE

Fig. 18. Brass Specimens After Exposure (Magnification = 10X).

(A)
AFTER EXPOSURE TO
0–5 μM PARTICLE
SIZE RANGE

(B)
AFTER EXPOSURE TO
0–30 μM PARTICLE
SIZE RANGE

(C)
AFTER EXPOSURE TO
0–80 μM PARTICLE
SIZE RANGE

Fig. 19. Aluminum Specimens After Contaminant Exposure (Magnification = 10X).

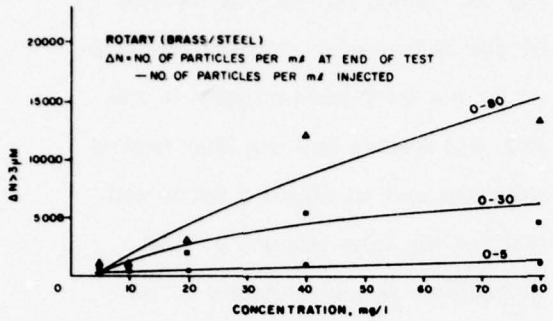

Fig. 20. Increase in No. of Particles Greater Than 3 Micrometres Due to Wear Debris Generated During Rotary (Brass/Steel Tests).

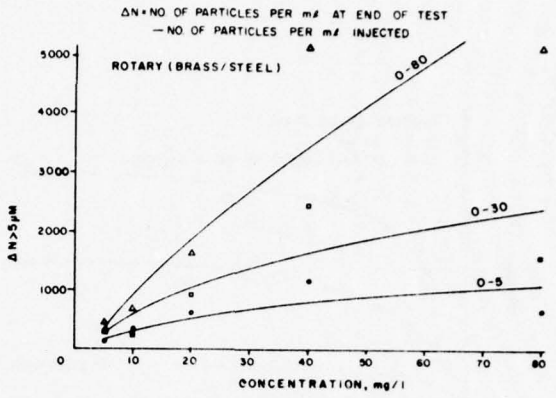

Fig. 21. Increase in No. of Particles Greater Than 5 Micrometres Due to Wear Debris Generated During Rotary (Brass/Steel) Tests.

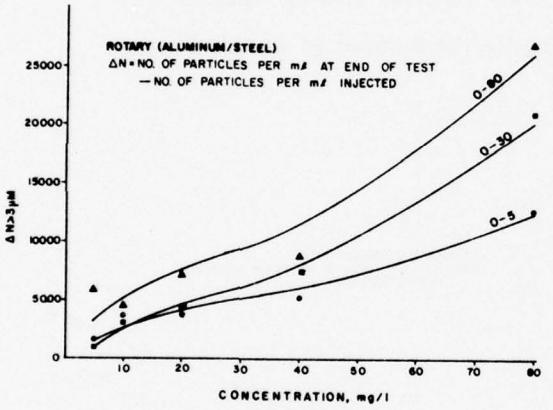

Fig. 22. Increase in No. of Particles Greater Than 3 Micrometres Due to Wear Debris Generated During Rotary (Aluminum/Steel) Tests.

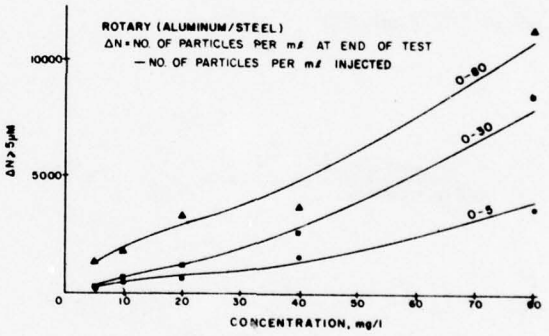

Fig. 23. Increase in No. of Particles Greater Than 5 Micrometres Due to Wear Debris Generated During Rotary (Aluminum/Steel) Tests.

contaminant during the wear action, which is why particle count analysis must be used with great care. It was felt that, during these tests, this situation would occur at about the 15-20 minute point of the test. In analyzing the Ferrographic density reading, however, it was realized that almost all of the significant wear occurred in the first seven minutes of the test. Therefore, the concentration of wear debris for the seven minute point and later were fairly constant. This phenomenon is illustrated by the results of the brass/steel test using 0-30

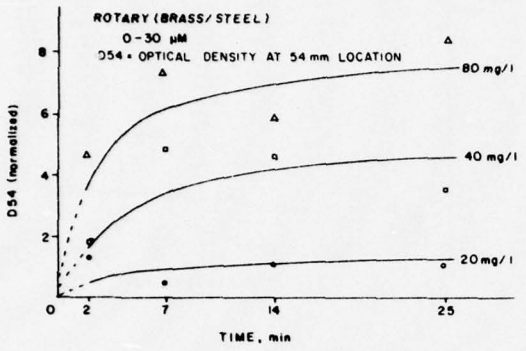

Fig. 24. Ferrographic Density (D54) versus Test Time for 0-30 Micrometre Injection During Rotary (Brass/Steel) Tests.

micrometre contaminant, as shown in Fig. 24. Since the wear as revealed by the Ferrographic densities had ceased by the seven minute point in the test, this reading and the later reading were averaged to obtain a better estimate of the total amount of wear. In addition, it was necessary to use different amounts of fluid when preparing Ferrograms due to the varying amounts of wear debris present. In order to place density readings on a common basis, all readings were normalized by dividing by the amount of sample fluid used in the analysis.

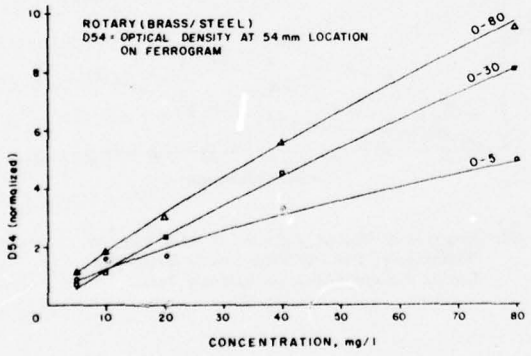

Fig. 25. Ferrographic Density (D54) versus Contaminant Concentration for Rotary (Brass/Steel) Tests.

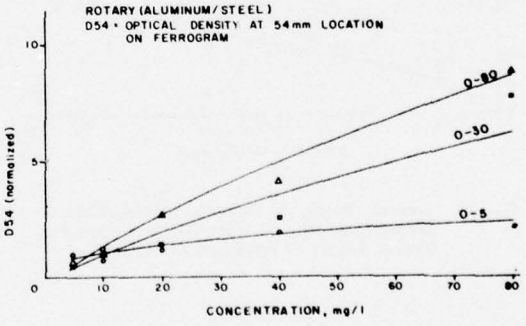

Fig. 26. Ferrographic Density (D54) versus Contaminant Concentration for Rotary (Aluminum/Steel) Tests.

The amount of wear as revealed by the Ferrographic density measured at the 54 mm location on the Ferrogram is shown in Figs. 25 and 26 for the brass/steel and aluminum/steel tests, respectively. The D54 measurement has been normalized to a consistent fluid

volume in these figures. In addition, as was noted earlier, the density readings represent the total amount of wear and were obtained by averaging the last three sample readings. In general, it can be observed that the magnitude of wear increases with both particle size and concentration of injected contaminant. Also, by comparing the wear which results using brass/steel and aluminum/steel, it can be noted that the brass/steel exhibited more wear when exposed to the 0-5 micrometre particle size range than the aluminum/steel combination. However, the aluminum/steel specimens reveal a greater amount of wear than brass/steel when exposed to the larger size range.

Through the use of the photographic accessories of the Bichromatic Microscope, pictures were made of the wear debris collected on each Ferrogram at the 54 mm location. Figures 27 through 31 show the wear debris deposit at 100X magnification from the tests conducted with the brass/steel specimens, while Figs. 32 through 36 reveal the nature of the same debris taken at 1000X magnification. The pictures were all taken at the 54 mm position on the appropriate Ferrogram. From the low power (100X) figures, it can be observed that the amount of wear debris increases with both increasing particle size and concentration. It is felt that these pictures are a definite aid in evaluating the density readings taken from the same position on the slide. The actual particle structure cannot be assessed from the low power figures; however, the particle strings become much longer and heavier as the amount of debris increases, revealing that most of the debris collected came from the mild steel specimen.

The high power pictures shown in Figs. 32 through 36 reveal the nature of the debris in much greater detail. In general, the particles of debris tend to become larger when larger particle size ranges were used. Also, there is very little evidence of cutting type wear debris (lathe type) within 0-5 micrometre contaminant exposed. However, when the mechanism was subjected to 0-30 micrometres, many hair-like cutting wear particles were observed. The cutting wear became even more severe in the face of 0-80 micrometre contaminant; however, the particles tend to be shorter and heavier than those resulting from a 0-30 micrometre exposure. In addition, very little brass particles were observed on the Ferrograms, although one of the surfaces was fabricated from brass material.

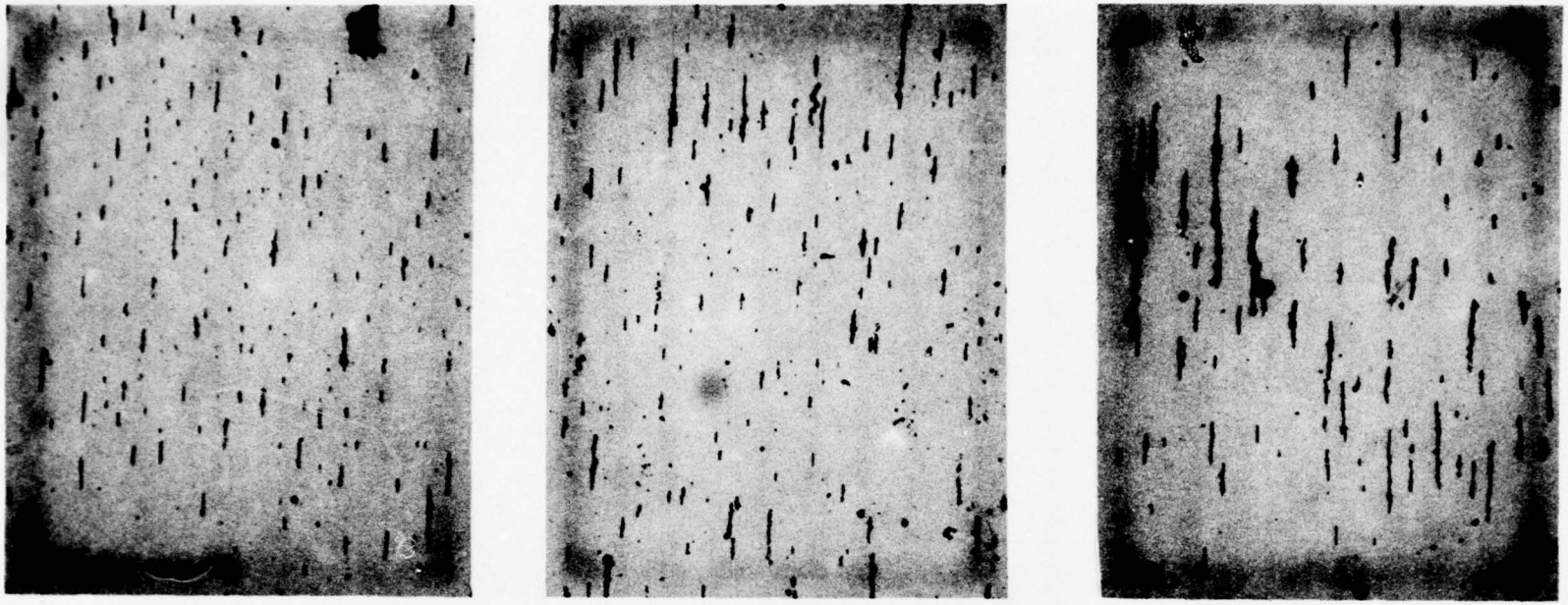

(a)
AFTER EXPOSURE TO
0-5 μM PARTICLE
SIZE RANGE

(b)
AFTER EXPOSURE TO
0-30 μM PARTICLE
SIZE RANGE

(c)
AFTER EXPOSURE TO
0-80 μM PARTICLE
SIZE RANGE

Fig. 27. Ferrograms of Wear Debris (54mm) from Brass on Steel Rotary Mechanism After Exposure to 5.0 mg/litre of Contaminant (Magnification = 100)

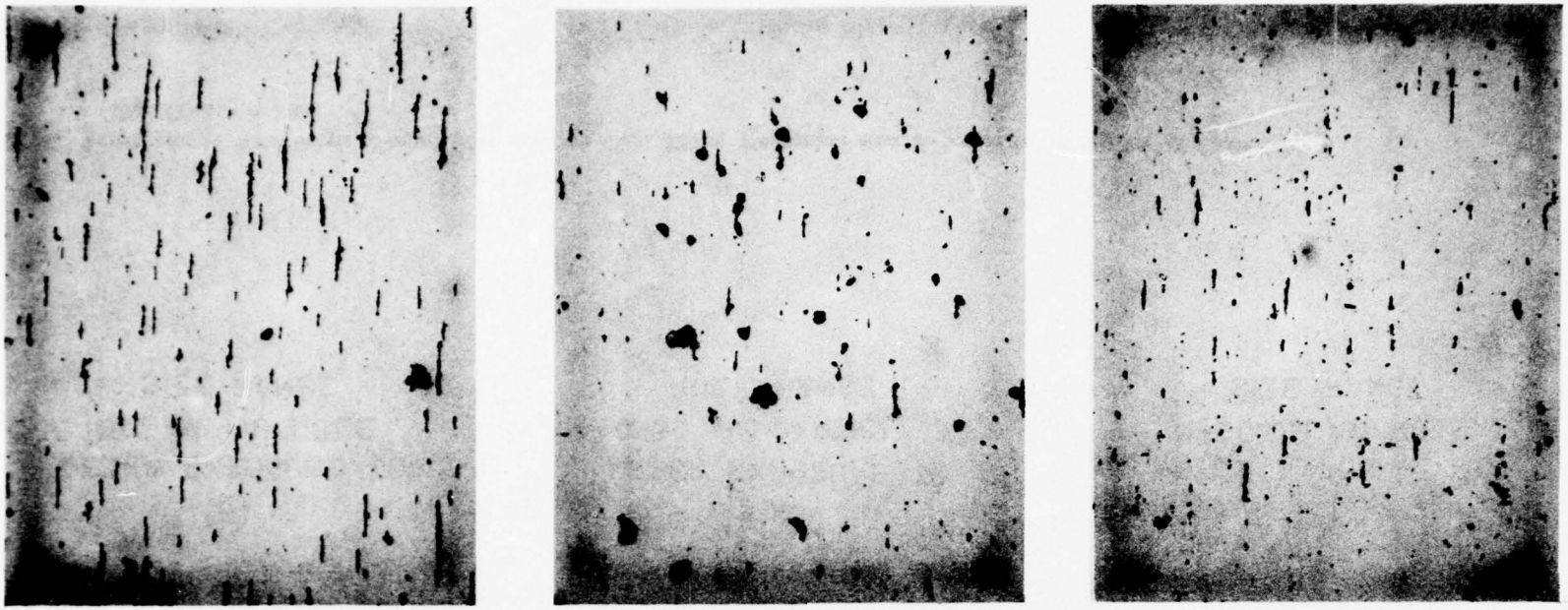

(a)
AFTER EXPOSURE TO
0-5 μM PARTICLE
SIZE RANGE

(b)
AFTER EXPOSURE TO
0-30 μM PARTICLE
SIZE RANGE

(c)
AFTER EXPOSURE TO
0-80 μM PARTICLE
SIZE RANGE

Fig. 28. Ferrograms of Wear Debris (54mm) from Brass on Steel Rotary Mechanism After Exposure to 10 mg/litre of Contaminant (Magnification = 100).

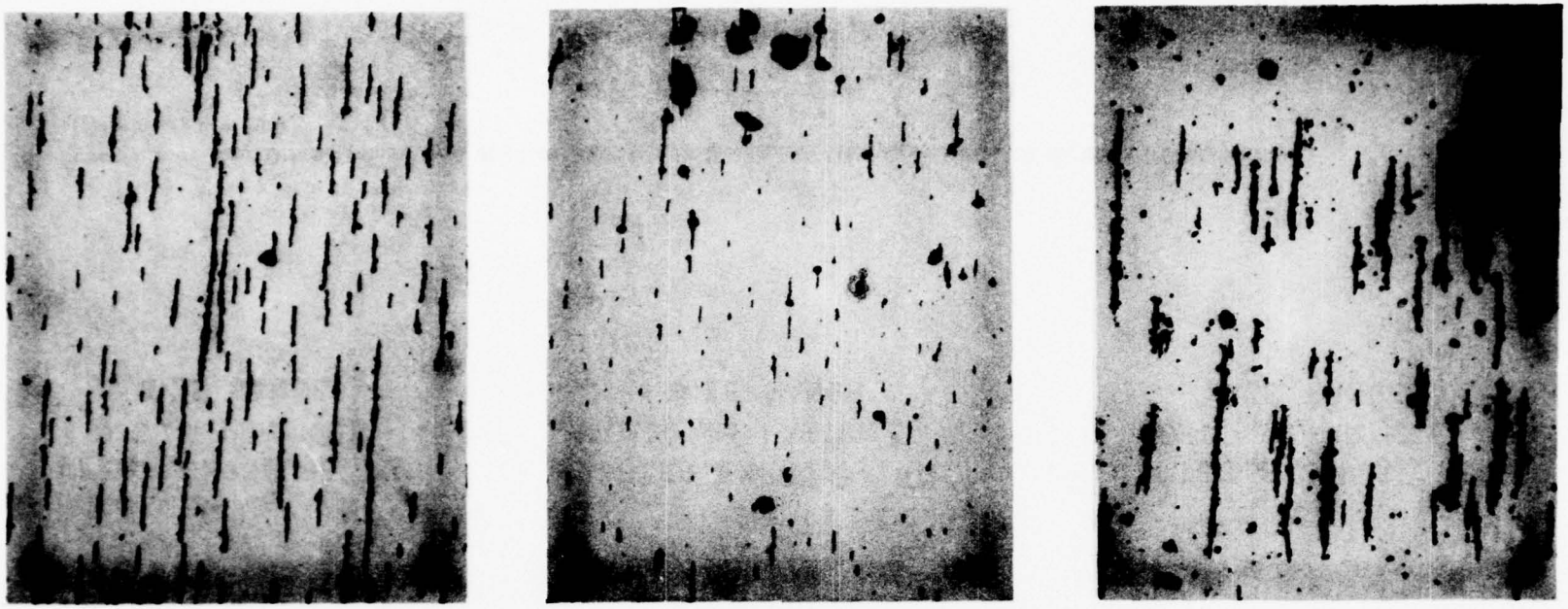

(a)
AFTER EXPOSURE TO
0-5 μM PARTICLE
SIZE RANGE

(b)
AFTER EXPOSURE TO
0-30 μM PARTICLE
SIZE RANGE

(c)
AFTER EXPOSURE TO
0-80 μM PARTICLE
SIZE RANGE

Fig. 29. Ferrograms of Wear Debris (54mm) from Brass on Steel Rotary Mechanism after Exposure to 20 mg/litre of Contaminant (Magnification = 100).

(a)
AFTER EXPOSURE TO
0-5 μM PARTICLE
SIZE RANGE

(b)
AFTER EXPOSURE TO
0-30 μM PARTICLE
SIZE RANGE

(c)
AFTER EXPOSURE TO
0-80 μM PARTICLE
SIZE RANGE

Fig. 30. Ferrograms of Wear Debris (54mm) from Brass on Steel Rotary Mechanism after Exposure to 40 mg/litre of Contaminant (Magnification = 100).

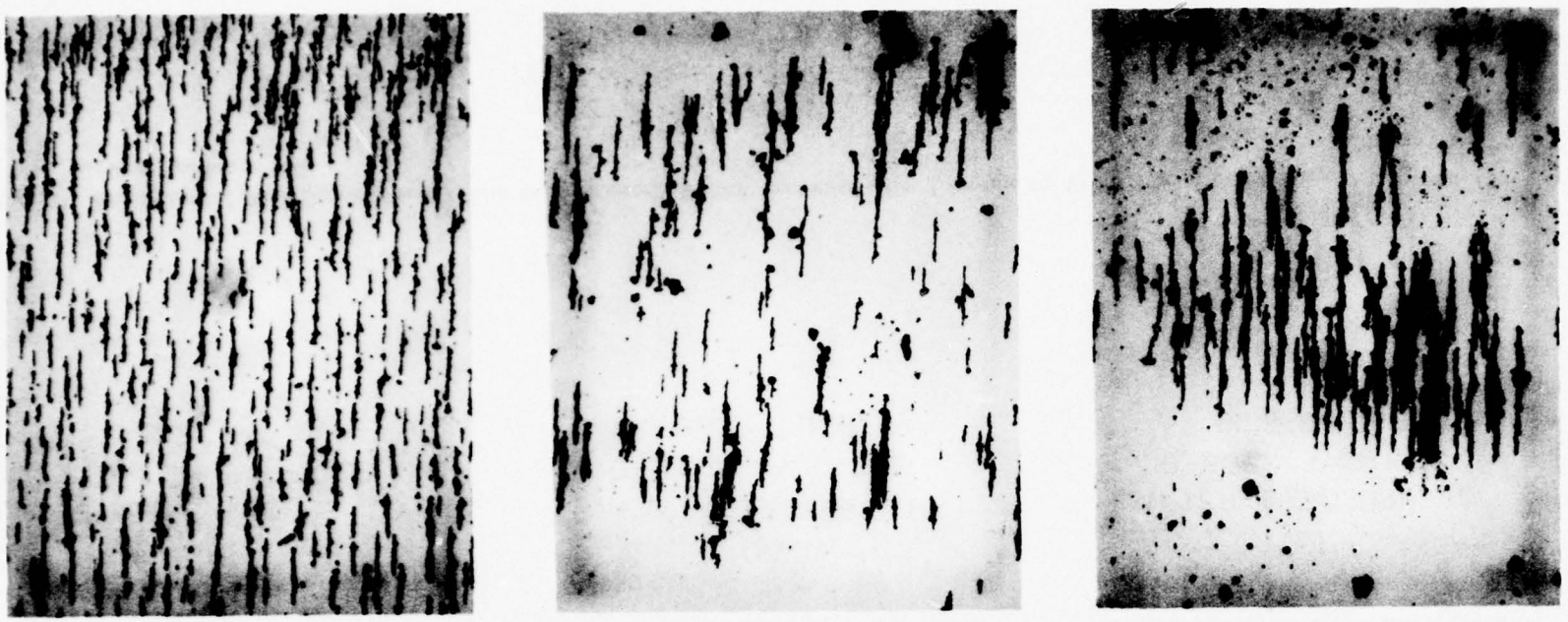

(a)
AFTER EXPOSURE TO
0-5 μM PARTICLE
SIZE RANGE

(b)
AFTER EXPOSURE TO
0-30 μM PARTICLE
SIZE RANGE

(c)
AFTER EXPOSURE TO
0-80 μM PARTICLE
SIZE RANGE

Fig. 31. Ferrograms of Wear Debris (54mm) from Brass on Steel Rotary Mechanism after Exposure to 80 mg/litre of Contaminant (Magnification = 100).

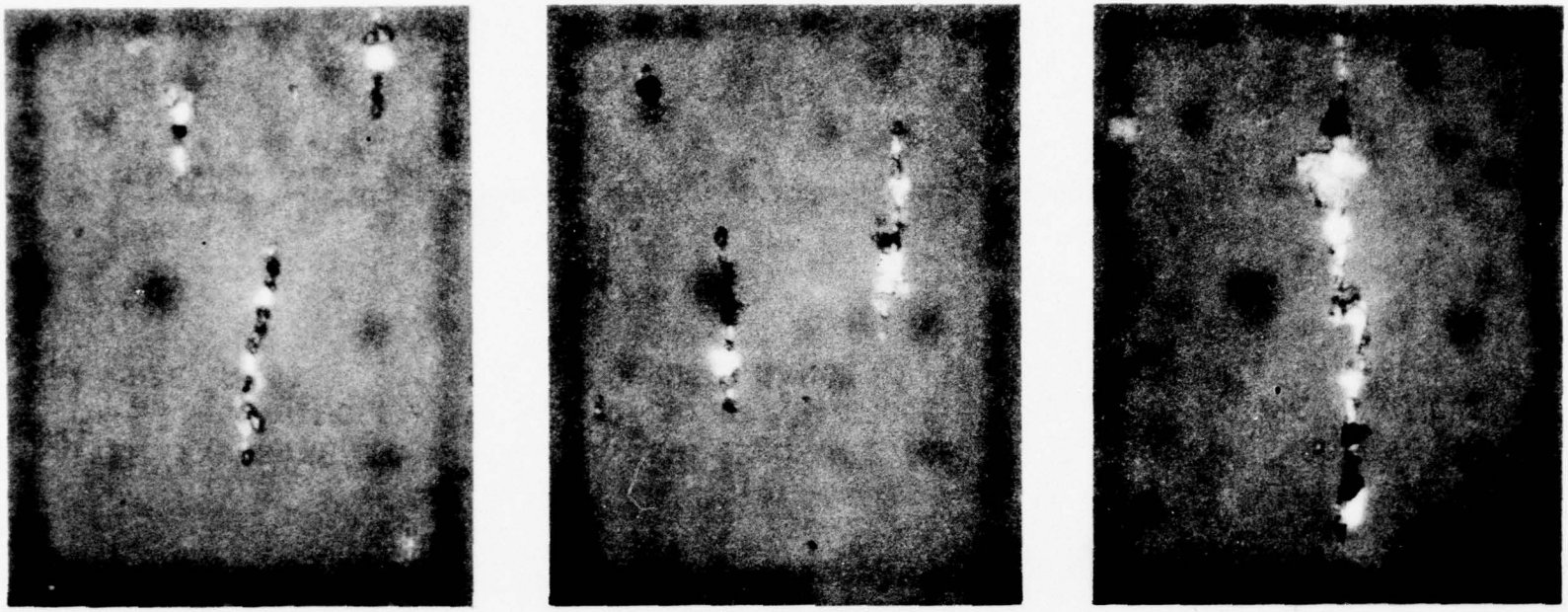

(A)
AFTER EXPOSURE TO
0–5 μM PARTICLE
SIZE RANGE

(B)
AFTER EXPOSURE TO
0–30 μM PARTICLE
SIZE RANGE

(C)
AFTER EXPOSURE TO
0–80 μM PARTICLE
SIZE RANGE

Fig. 32. Ferrograms of Wear Debris (54mm) from Brass on Steel Rotary Mechanism after Exposure to 5 mg/litre of Contaminant (Magnification 1000X).

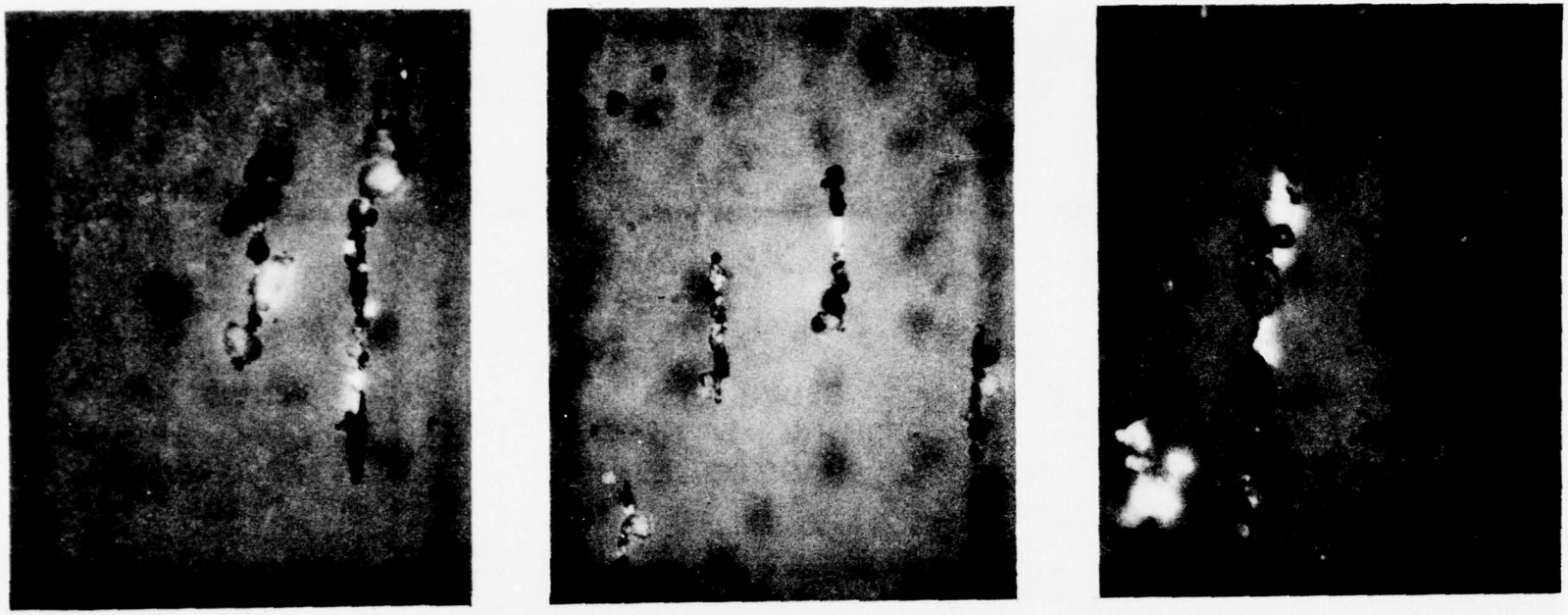

(A)
AFTER EXPOSURE TO
0–5 μM PARTICLE
SIZE RANGE

(B)
AFTER EXPOSURE TO
0–30 μM PARTICLE
SIZE RANGE

(C)
AFTER EXPOSURE TO
0–80 μM PARTICLE
SIZE RANGE

Fig. 33. Ferrograms of Wear Debris (54mm) from Brass on Steel Rotary Mechanism after Exposure to 10 mg/litre of Contaminant (Magnification 1000X).

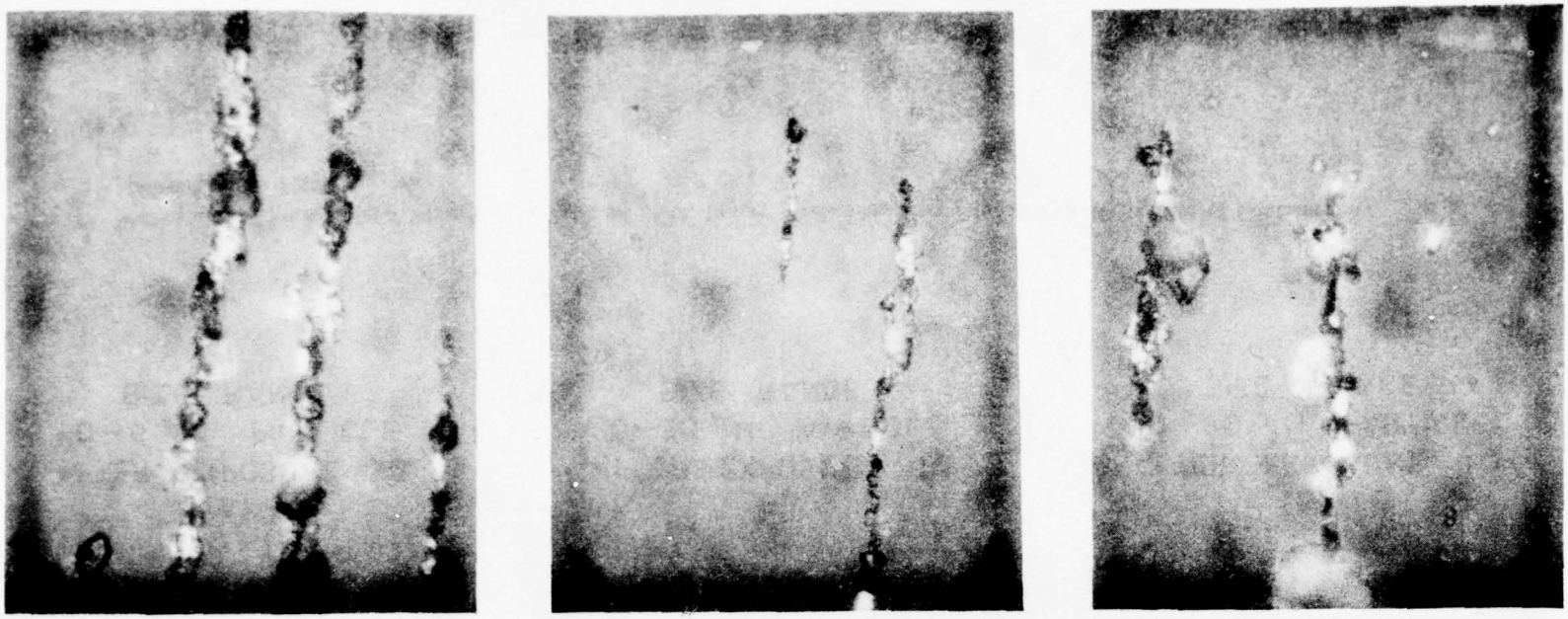

(A)
AFTER EXPOSURE TO
0–5 μM PARTICLE
SIZE RANGE

(B)
AFTER EXPOSURE TO
0–30 μM PARTICLE
SIZE RANGE

(C)
AFTER EXPOSURE TO
0–80 μM PARTICLE
SIZE RANGE

Fig. 34. Ferrograms of Wear Debris (54mm) from Brass on Steel Rotary Mechanism after Exposure to 20 mg/litre of Contaminant (Magnification 1000X).

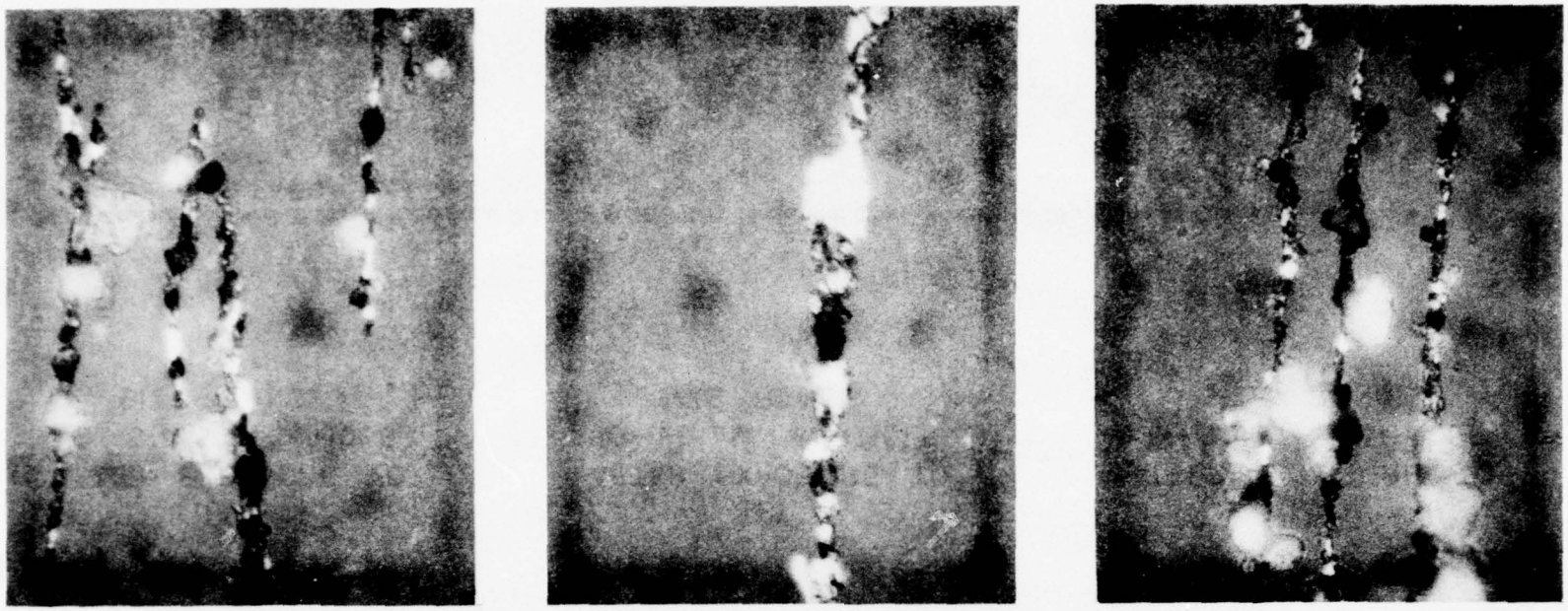

(A)
AFTER EXPOSURE TO
0—5 μM PARTICLE
SIZE RANGE

(B)
AFTER EXPOSURE TO
0—30 μM PARTICLE
SIZE RANGE

(C)
AFTER EXPOSURE TO
0—80 μM PARTICLE
SIZE RANGE

Fig. 35. Ferrograms of Wear Debris (54mm) from Brass on Steel Rotary Mechanism after Exposure to 40 mg/litre of Contaminant (Magnification 1000X).

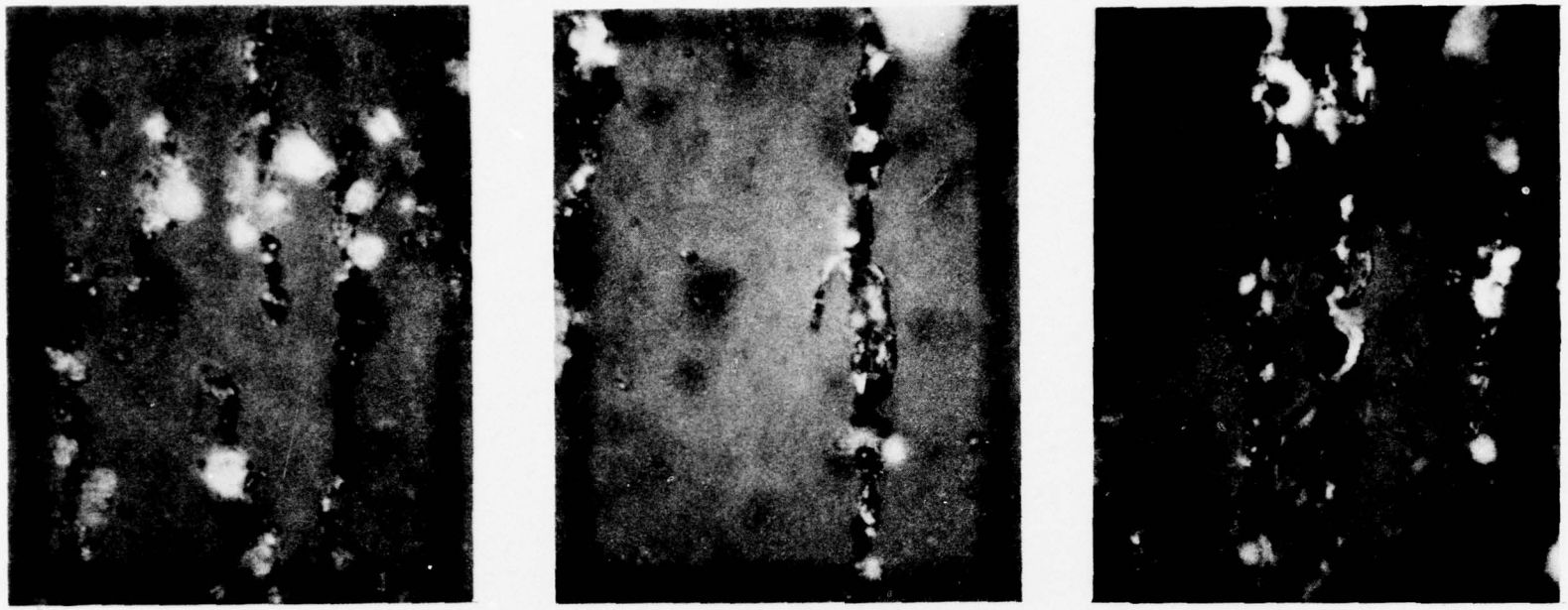

(A)
AFTER EXPOSURE TO
0–5 μM PARTICLE
SIZE RANGE

(B)
AFTER EXPOSURE TO
0–30 μM PARTICLE
SIZE RANGE

(C)
AFTER EXPOSURE TO
0–80 μM PARTICLE
SIZE RANGE

Fig. 36. Ferrograms of Wear Debris (54mm) from Brass on Steel Rotary Mechanism after Exposure to 80 mg/litre of Contaminant (Magnification 1000X).

The micro-photographs for the aluminum/steel tests are shown in Figs. 37 through 41 at low power (100X) and Figs. 42 through 46 taken at high power (100X). In general, the same comments made in relation to the debris from the brass/steel tests can be applied to the aluminum/steel test results. Very few aluminum particles could be identified in the debris collected. However, the nature of the wear debris is very definitely affected by the particle size and concentration of the test contaminant.

(a)
AFTER EXPOSURE TO
0-5 μM PARTICLE
SIZE RANGE

(b)
AFTER EXPOSURE TO
0-30 μM PARTICLE
SIZE RANGE

(c)
AFTER EXPOSURE TO
0-80 μM PARTICLE
SIZE RANGE

Fig. 37. Ferrograms of Wear Debris (54mm) from Aluminum on Steel Rotary Mechanism after Exposure to 5 mg/litre of Contaminant (Magnification = 100).

(a)
AFTER EXPOSURE TO
0-5 μM PARTICLE
SIZE RANGE

(b)
AFTER EXPOSURE TO
0-30 μM PARTICLE
SIZE RANGE

(c)
AFTER EXPOSURE TO
0-80 μM PARTICLE
SIZE RANGE

Fig. 38. Ferrograms of Wear Debris (54mm) from Aluminum on Steel Rotary Mechanism after Exposure to 10 mg/litre of Contaminant (Magnification = 100).

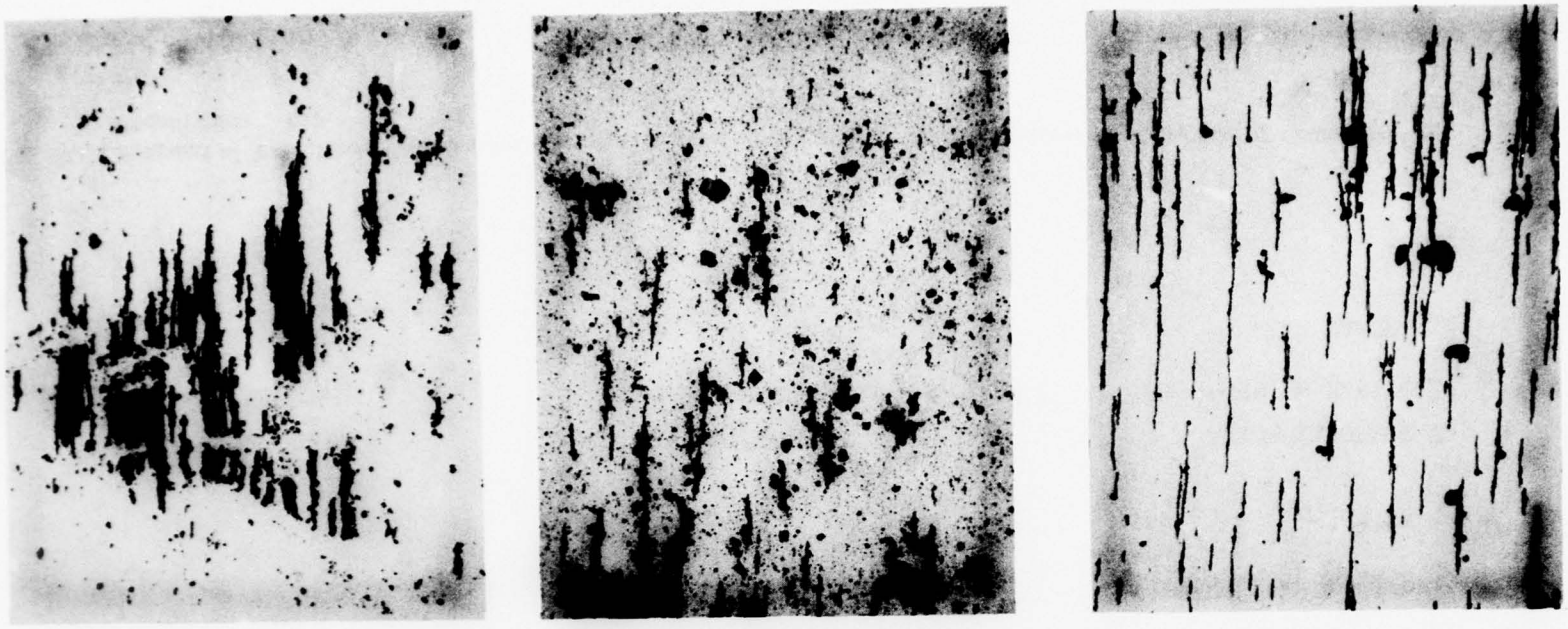

(a)
AFTER EXPOSURE TO
0-5 μM PARTICLE
SIZE RANGE

(b)
AFTER EXPOSURE TO
0-30 μM PARTICLE
SIZE RANGE

(c)
AFTER EXPOSURE TO
0-80 μM PARTICLE
SIZE RANGE

Fig. 39. Ferrograms of Wear Debris (54mm) from Aluminum on Steel Rotary Mechanism after Exposure to 20 mg/litre of Contaminant (Magnification = 100).

(a)
AFTER EXPOSURE TO
0-5 μM PARTICLE
SIZE RANGE

(b)
AFTER EXPOSURE TO
0-30 μM PARTICLE
SIZE RANGE

(c)
AFTER EXPOSURE TO
0-80 μM PARTICLE
SIZE RANGE

Fig. 40. Ferrograms of Wear Debris (54mm) from Aluminum on Steel Rotary Mechanism after Exposure to 40 mg/litre of Contaminant (Magnification = 100).

(a)
AFTER EXPOSURE TO
0-5 μM PARTICLE
SIZE RANGE

(b)
AFTER EXPOSURE TO
0-30 μM PARTICLE
SIZE RANGE

(c)
AFTER EXPOSURE TO
0-80 μM PARTICLE
SIZE RANGE

Fig. 41. Ferrograms of Wear Debris (54mm) from Aluminum on Steel Rotary Mechanism after Exposure to 80 mg/litre of Contaminant (Magnification = 100).

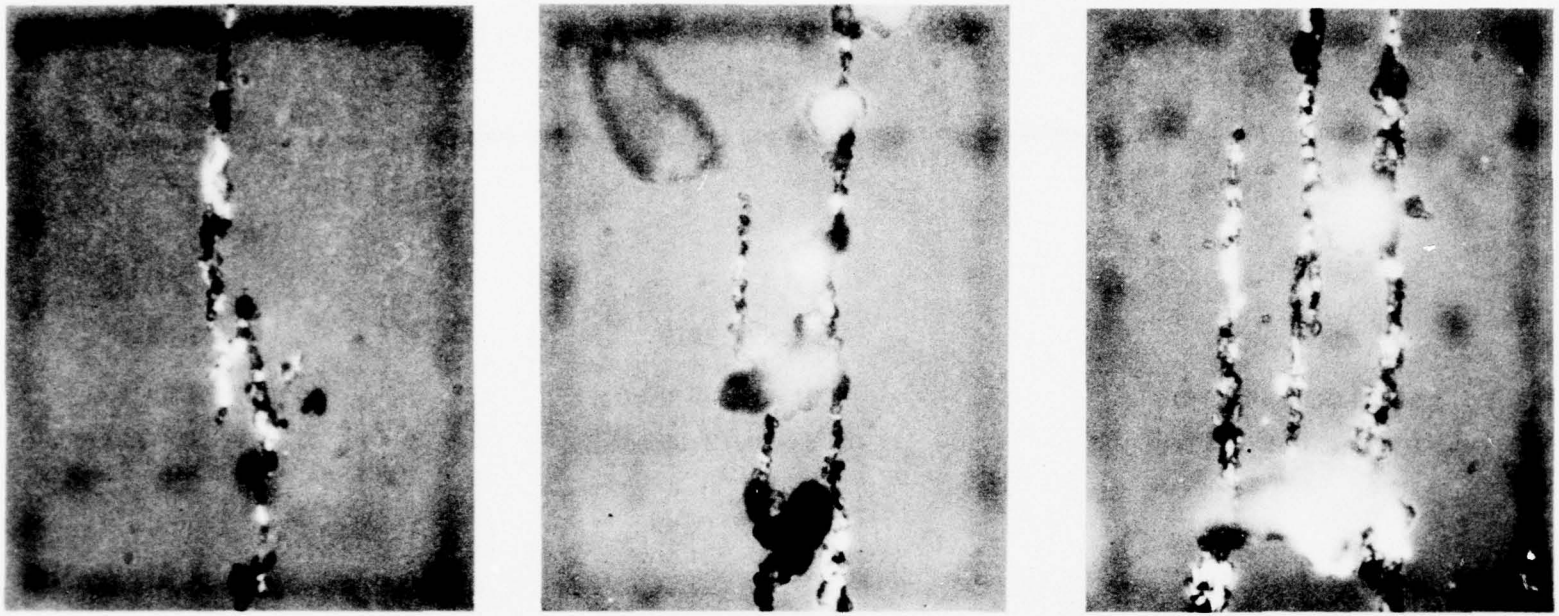

(a)
AFTER EXPOSURE TO
0-5 μM PARTICLE
SIZE RANGE

(b)
AFTER EXPOSURE TO
0-30 μM PARTICLE
SIZE RANGE

(c)
AFTER EXPOSURE TO
0-80 μM PARTICLE
SIZE RANGE

Fig. 42. Ferrograms of Wear Debris (54mm) from Aluminum on Steel Rotary Mechanism After Exposure to 5 mg/litre of Contaminant (Magnification = 1000).

(a)
AFTER EXPOSURE TO
0-5 μM PARTICLE
SIZE RANGE

(b)
AFTER EXPOSURE TO
0-30 μM PARTICLE
SIZE RANGE

(c)
AFTER EXPOSURE TO
0-80 μM PARTICLE
SIZE RANGE

Fig. 43. Ferrograms of Wear Debris (54mm) from Aluminum on Steel Rotary Mechanism after Exposure to 10 mg/litre of Contaminant (Magnification = 1000).

(a)
AFTER EXPOSURE TO
0-5 μM PARTICLE
SIZE RANGE

(b)
AFTER EXPOSURE TO
0-30 μM PARTICLE
SIZE RANGE

(c)
AFTER EXPOSURE TO
0-80 μM PARTICLE
SIZE RANGE

Fig. 44. Ferrograms of Wear Debris (54mm) from Aluminum on Steel Rotary Mechanism after Exposure to 20 mg/litre of Contaminant (Magnification = 1000).

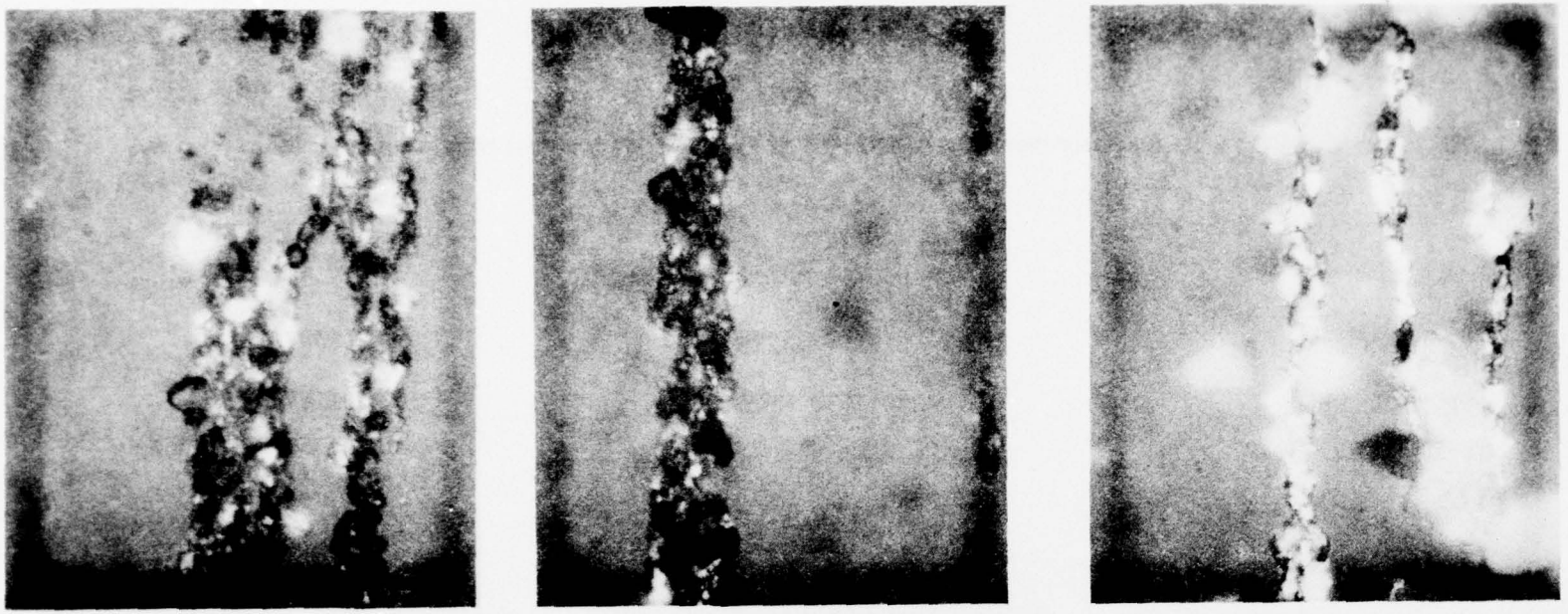

(a)
AFTER EXPOSURE TO
0-5 μM PARTICLE
SIZE RANGE

(b)
AFTER EXPOSURE TO
0-30 μM PARTICLE
SIZE RANGE

(c)
AFTER EXPOSURE TO
0-80 μM PARTICLE
SIZE RANGE

Fig. 45. Ferrograms of Wear Debris (54mm) from Aluminum on Steel Rotary Mechanism after Exposure to 40 mg/litre of Contaminant (Magnification = 1000).

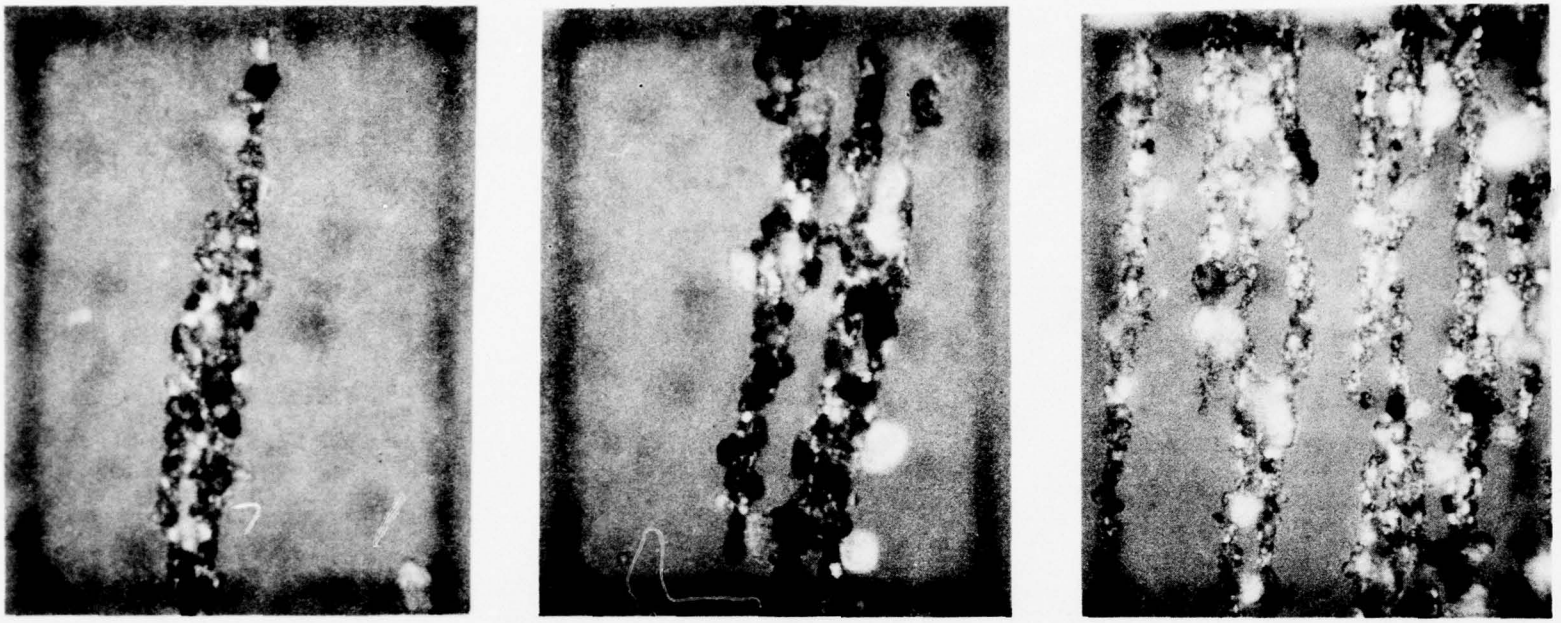

(a)
AFTER EXPOSURE TO
0-5 μM PARTICLE
SIZE RANGE

(b)
AFTER EXPOSURE TO
0-30 μM PARTICLE
SIZE RANGE

(c)
AFTER EXPOSURE TO
0-80 μM PARTICLE
SIZE RANGE

Fig. 46. Ferrograms of Wear Debris (54mm) from Aluminum on Steel Rotary Mechanism after Exposure to 80 mg/litre of Contaminant (Magnification = 1000).

CHAPTER VII

DESCRIPTION OF THE LINEAR MECHANISM

The linear mechanism used in this study simulates the type of surface contact existing in hydraulic spool valves or the pistons in a piston pump or motor. The design used, Fig. 47, consists of a double-ended steel spool and two cast iron bore blocks, both installed in a housing which provides proper alignment. The symmetry of the interior chamber provides a force balance at all chamber pressures, making the spool drive hardware easier and simpler to construct and more controllable.

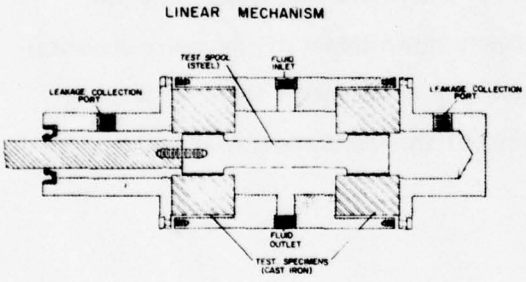

Fig. 47. Schematic of Linear Mechanism.

The mechanism housing has four ports, equally spaced around the mid-diameter, of which two opposing ports were used for inlets and the remaining two ports for outlets. This selection of port usage created yet another force balance, this time on the lateral axis of the space, eliminating the side loading that would have been experienced with asymmetric porting.

The end caps of the mechanism are used to clamp the bore blocks to the housing. The end caps were constructed in such a way as to provide a closed-space leakage collection chamber, which could be piped back to the system reservoir. This allowed for maintaining a constant volume in the test system as well as providing a convenient means of measuring the leakage flow rate.

Spool cycling was accomplished by an eccentric driven linkage connected to the spool through two linear bearings. The linear bearings were essential to maintain a smooth cycling action with the consistency that was needed. The drive units cycling rate could be varied from five cycles per minute to 85 cycles per minute.

The test specimens were manufactured in matched sets, consisting of a steel spool and two cast iron bore specimens. The bore pieces were machined from the same stock and then parted and the faces ground perpendicular to the hole. The bores were honed together to a nominal .500" diameter. The steel spool was then constructed from 1020 mild steel. It was cylindrically ground to match the bore specimens but with the spool diameter being 25 micrometres less than the bore diameter.

The fluid test system used was the same as that for the rotary mechanism tests but with one modification. A valve was installed immediately downstream of the test mechanism to allow pressure adjustment under constant flow condition. This meant that the pressure could be adjusted to any level up to the 1000 psi limit of the test system itself.

TEST CONDITIONS AND PARAMETERS

As mentioned, the clearance of the spool and bore diameters was made to be 25 micrometres. This clearance was arrived at after considerable experimentation with the mechanism and the physical limitations of it. It was found that a 25 micrometre clearance was the minimum that could be obtained with adequate repeatability of both the fabrication and the performance of the mechanism. The 25 micrometres is comparable with the clearance used in the rotary mechanism tests.

There were several parameters that were bounded in scope by the test system, and it would have required massive modifications to extend the parameter ranges. The cycle rate was limited by the driver's maximum rate of 85 cycles per minute. The maximum was

chosen because it was approaching operating velocities found in spool valves and also for the increased number of cycles that would be obtained in a reasonable length of test. One thousand psi was chosen for the test pressure, since it was the upper limit of the test stand's performance and because it approached typical component parameters. One other consideration in pressure setting was the leakage rate, which needed to be large enough to measure.

The flow rate maintained through the fixtures was 2.5 to 3 GPM. It was found that this flow rate was adequate to keep the injected contaminant in suspension. Operating at the above flow rate and pressure, unfortunately, posed a minor limitation on the system temperature. The characteristics of the system and the water temperature were such that it was necessary to maintain a system temperature of 120° F. Other than the above-mentioned parameter, the tests were similar to the rotary in all respects, including length and sample point.

TEST PROCEDURE

The following is an outline of the test procedure used in the linear mechanism tests:

1. Install test specimens in fixture, taking care in assuring proper alignment.

2. Circulate fluid through fixture with control filters ($Q > 3$ GPM) in the circuit and maintain 1000 psi pressure in the mechanism until system temperature reaches 120° F.

3. Start spool cycling at 85 cycles per minute.

4. Measure the leakage flow every ten minutes and continue cycling until four flow readings remain constant or until four hours have passed.

5. Block system filters from circuit, continue cycling at 85 cycles per minute, 1000 psi, and more than 3 GPM flow through the mechanism. Inject desired amount of contaminant to establish 5 mg/litre concentration.

6. Obtain samples and record leakage flow at 2, 7, 14, 25, and 45 minutes.

7. Return system control filters to the circuit and operate for 45 minutes to clean system fluid.

8. Repeat Steps 5-7 for 10, 20, 40, and 80 mg/litre concentrations.

9. Repeat Steps 1-8 for particle size distributions and 0-80 micrometre dust classified from AC Fine Test Dust.

TEST RESULTS

As was the case with the rotary mechanism tests, samples obtained during the linear mechanism tests were analyzed with both particle counting techniques and Ferrographic methods. Particle counting was accomplished with an automatic counter, which was calibrated to measure the number of particles per millilitre greater than 3, 5, 10, 20, and 30 micrometres in accordance with the "American National Standard Method for Calibration of Liquid Automatic Particle Counters Using AC Fine Test Dust (ANSI B93.28-1973)" [17]. The increase in the particle concentration was obtained by subtracting the particle concentration of the injected contaminant from the counts measured at the conclusion of each test. The particle size distributions of the various particle size ranges used in these tests were identical to those of the rotary mechanism tests.

The increase in particle concentration during the tests using 0-5 micrometre contaminant is shown in Fig. 48 for sizes greater than 3, 5, and 10. The increase in particles greater than 20 and 30 micrometres was insignificant. The particle concentration increase during the 0-30 and 0-80 micrometre tests on the linear mechanism are shown in Figs. 49 and 50, respectively.

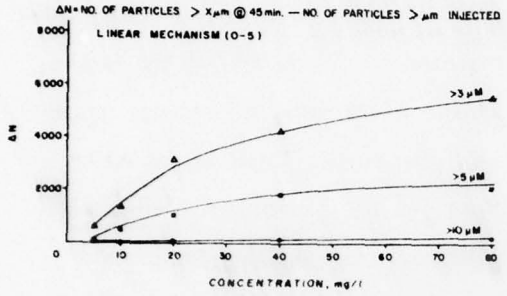

Fig. 48. Particle Count Analysis of Linear Mechanism Tests (0-5).

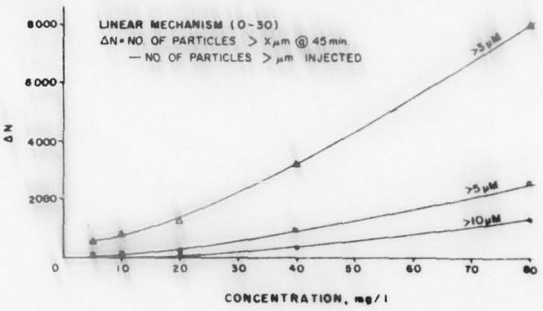

Fig. 49. Particle Count Analysis of Linear Mechanism Tests (0-30).

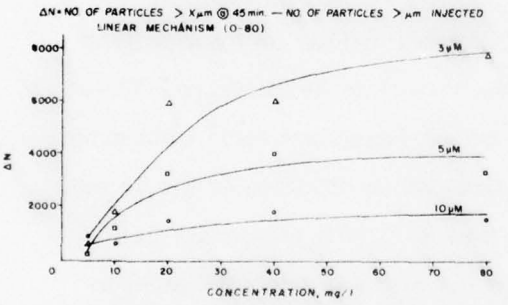

Fig. 50. Particle Count Analysis of Linear Mechanism Tests (0-80).

It should be noted from these figures that the trend of contaminant concentration buildup during the 0-5 and 0-80 micrometre tests were very similar.

From previous work in valve contaminant sensitivity, the fact that the particle size range which had an upper size limit close to the actual clearance produced vastly different results from those observed for other size ranges is not surprising. For example, in a spool valve, the force required to move the spool will be influenced by the concentration and particle size distribution of any entrained contaminant. When measuring this relationship, it normally will be found that one particular size range will have a more significant effect than smaller or larger sizes. Since this is usually attributed to a wedging action of critical size particles which are close to the size of the clearance, an increased wear rate should be expected at that size.

The normalized density reading obtained from Ferrograms of the linear mechanism tests are shown in Fig. 51. Of particular interest here is the fact that a significant amount of wear debris was measured during the 0-30 test over that observed in either the 0-5 or 0-80 tests. In fact, the 0-80 results were only slightly higher than those obtained during the test using 0-5 micrometre particle size range. This phenomenon again agrees with the logic that a critical size contaminant will cause more wedging action and hence more destruction than smaller or larger contaminant sizes.

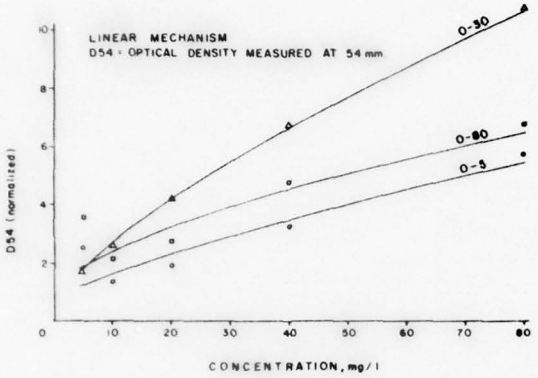

Fig. 51. Ferrographic Densities (D54) from Linear Mechanism Tests.

Micro-photographs of the Ferrograms associated with the linear mechanism tests are shown in Figs. 52 through 56 at a magnification of 100X and in Figs. 57 through 61 at 1000X. In general, the low power (100X) figures show the nature of the debris. There are definitely more cutting wear particles in evidence on the Ferrograms made from samples taken during the 0-30 micrometre exposure. The particles which deposited at the 54 mm location appear to be slightly larger in the 0-80 tests than in the 0-5 micrometre test, but neither of these is as large as those obtained when the mechanism was subjected to 0-30 micrometres.

When the results of the linear mechanism tests are compared to those of the rotary mechanism tests, it can be seen that more debris was generated with all particle size ranges at 5 mg/litre in the linear than in the rotary. This same trend can be observed from the plots of Ferrogram densities versus concentration at the other particle size ranges.

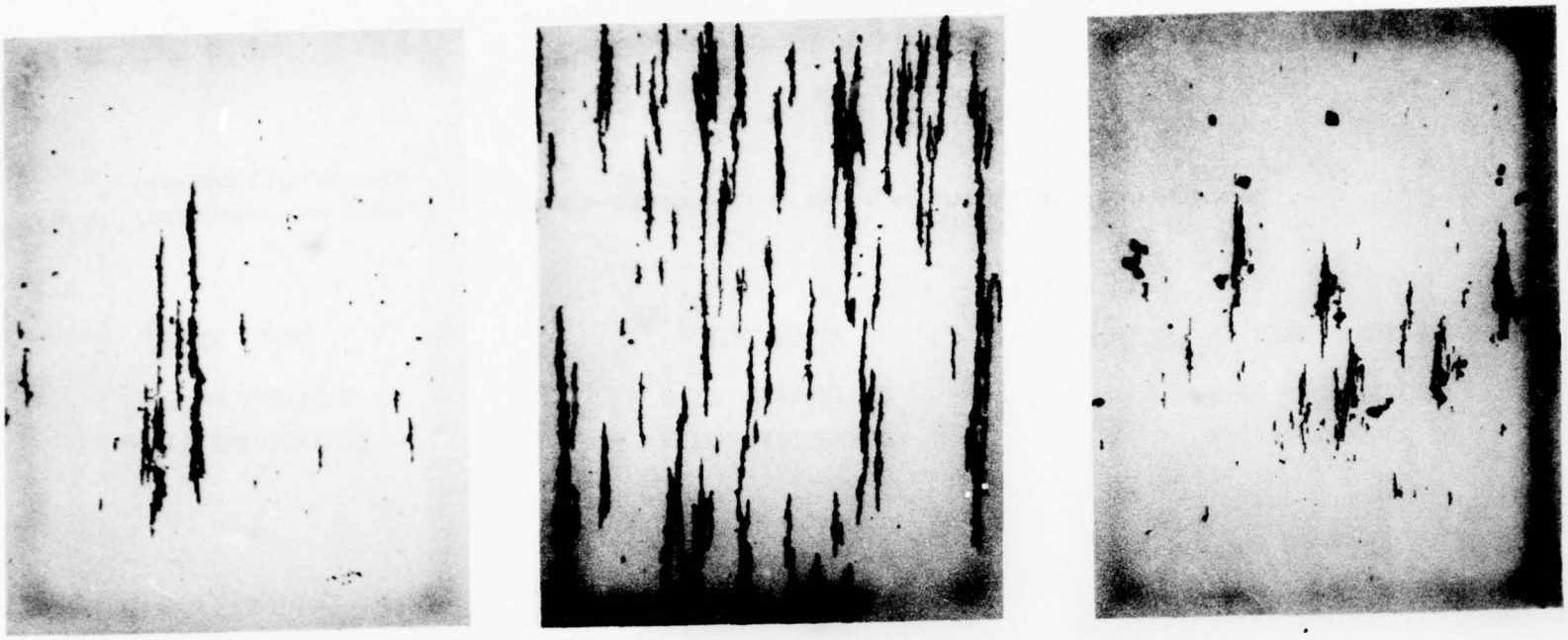

(a)
AFTER EXPOSURE TO
0-5 μM PARTICLE
SIZE RANGE

(b)
AFTER EXPOSURE TO
0-30 μM PARTICLE
SIZE RANGE

(c)
AFTER EXPOSURE TO
0-80 μM PARTICLE
SIZE RANGE

Fig. 52. Ferrograms of Wear Debris (54mm) from Linear Mechanism (Cast Iron–Steel) after Exposure to 5 mg/litre of Contaminant (Magnification = 100).

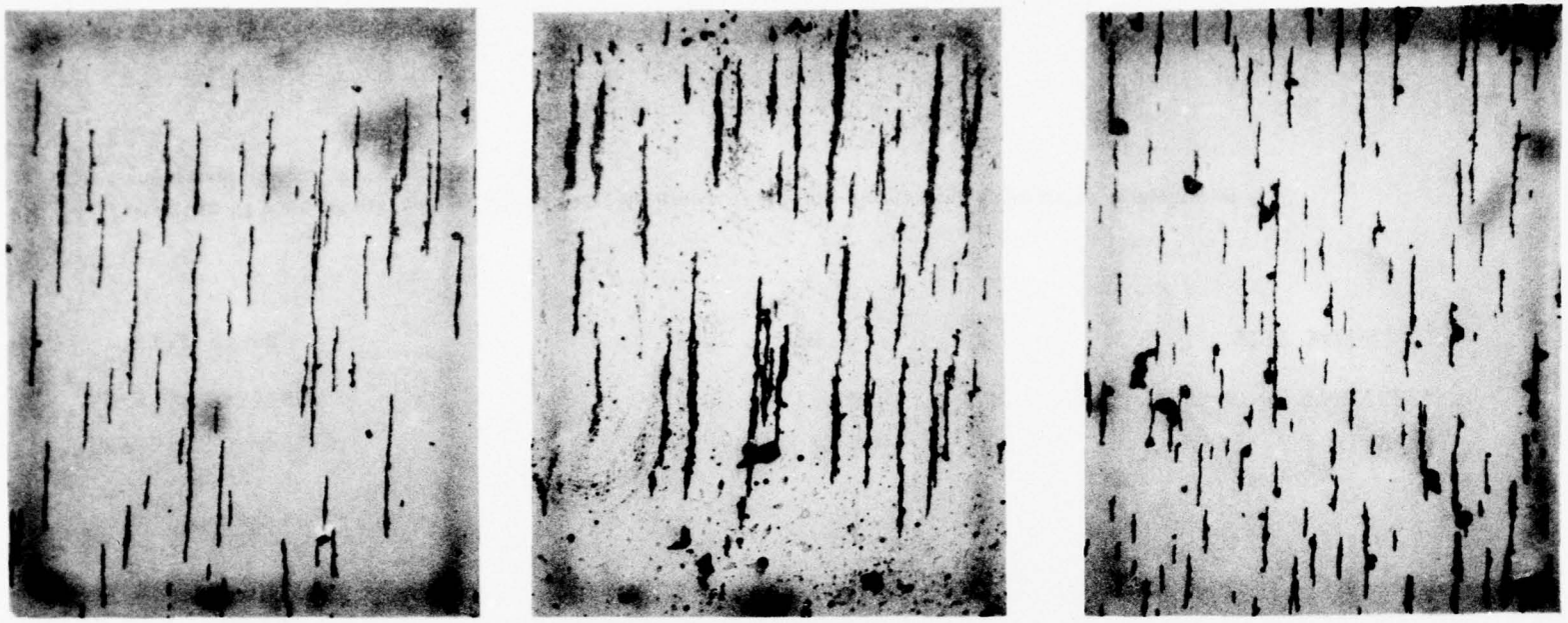

(a)
AFTER EXPOSURE TO
0-5 μM PARTICLE
SIZE RANGE

(b)
AFTER EXPOSURE TO
0-30 μM PARTICLE
SIZE RANGE

(c)
AFTER EXPOSURE TO
0-80 μM PARTICLE
SIZE RANGE

Fig. 53. Ferrograms of Wear Debris (54mm) from Linear Mechanism (Cast Iron–Steel) after Exposure to 10 mg/litre of Contaminant (Magnification = 100).

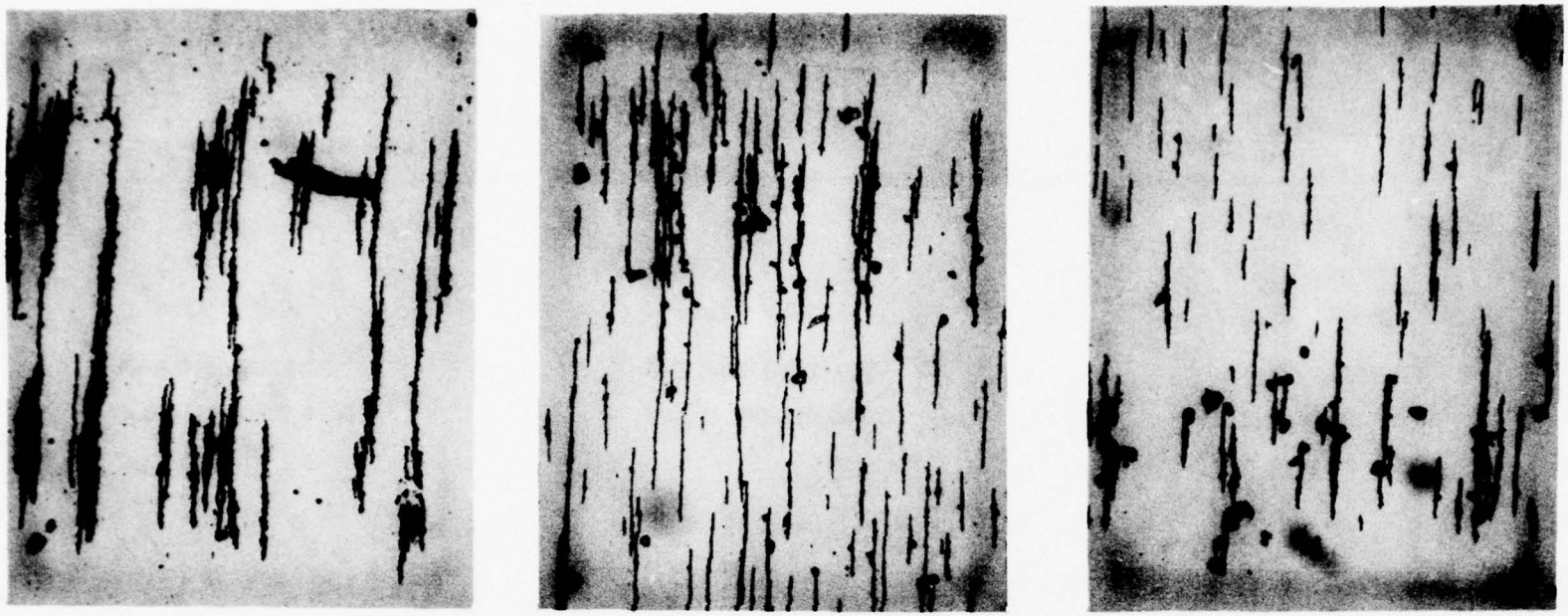

(a)
AFTER EXPOSURE TO
0-5 μM PARTICLE
SIZE RANGE

(b)
AFTER EXPOSURE TO
0-30 μM PARTICLE
SIZE RANGE

(c)
AFTER EXPOSURE TO
0-80 μM PARTICLE
SIZE RANGE

Fig. 54. Ferrograms of Wear Debris (54mm) from Linear Mechanism (Cast Iron–Steel) after Exposure to 20 mg/litre of Contaminant (Magnification = 100).

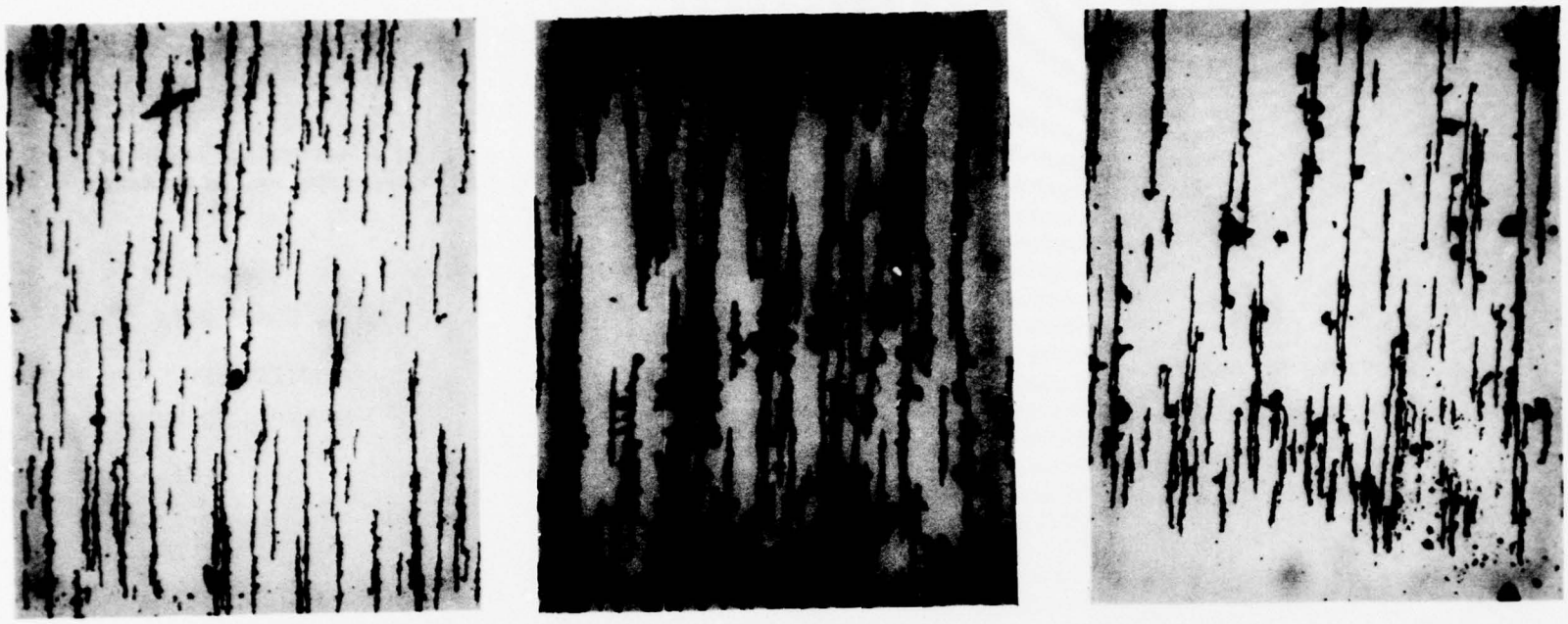

(a)
AFTER EXPOSURE TO
0-5 μM PARTICLE
SIZE RANGE

(b)
AFTER EXPOSURE TO
0-30 μM PARTICLE
SIZE RANGE

(c)
AFTER EXPOSURE TO
0-80 μM PARTICLE
SIZE RANGE

Fig. 55. Ferrograms of Wear Debris (54mm) from Linear Mechanism (Cast Iron–Steel) after Exposure to 40 mg/litre of Contaminant (Magnification = 100).

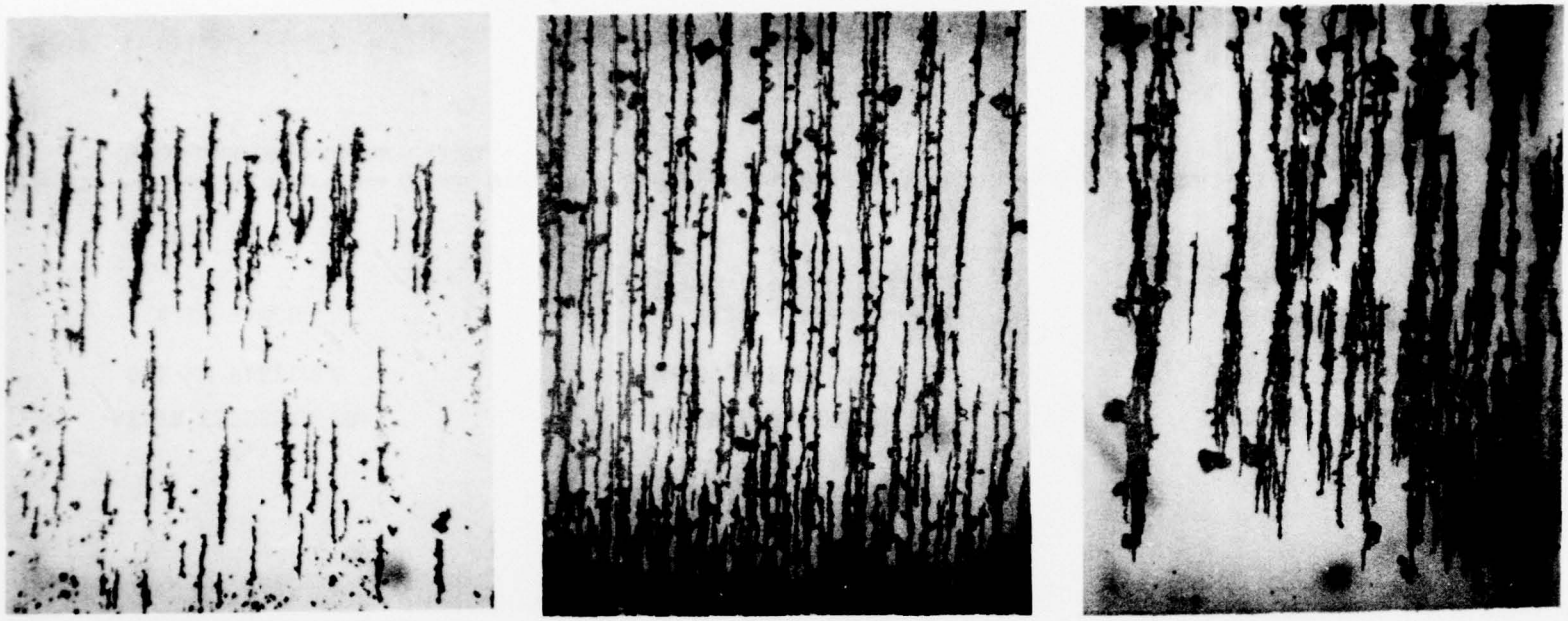

(a)
AFTER EXPOSURE TO
0-5 μM PARTICLE
SIZE RANGE

(b)
AFTER EXPOSURE TO
0-30 μM PARTICLE
SIZE RANGE

(c)
AFTER EXPOSURE TO
0-80 μM PARTICLE
SIZE RANGE

Fig. 56. Ferrograms of Wear Debris (54mm) from Linear Mechanism (Cast Iron–Steel) after Exposure to 80 mg/litre of Contaminant (Magnification = 100).

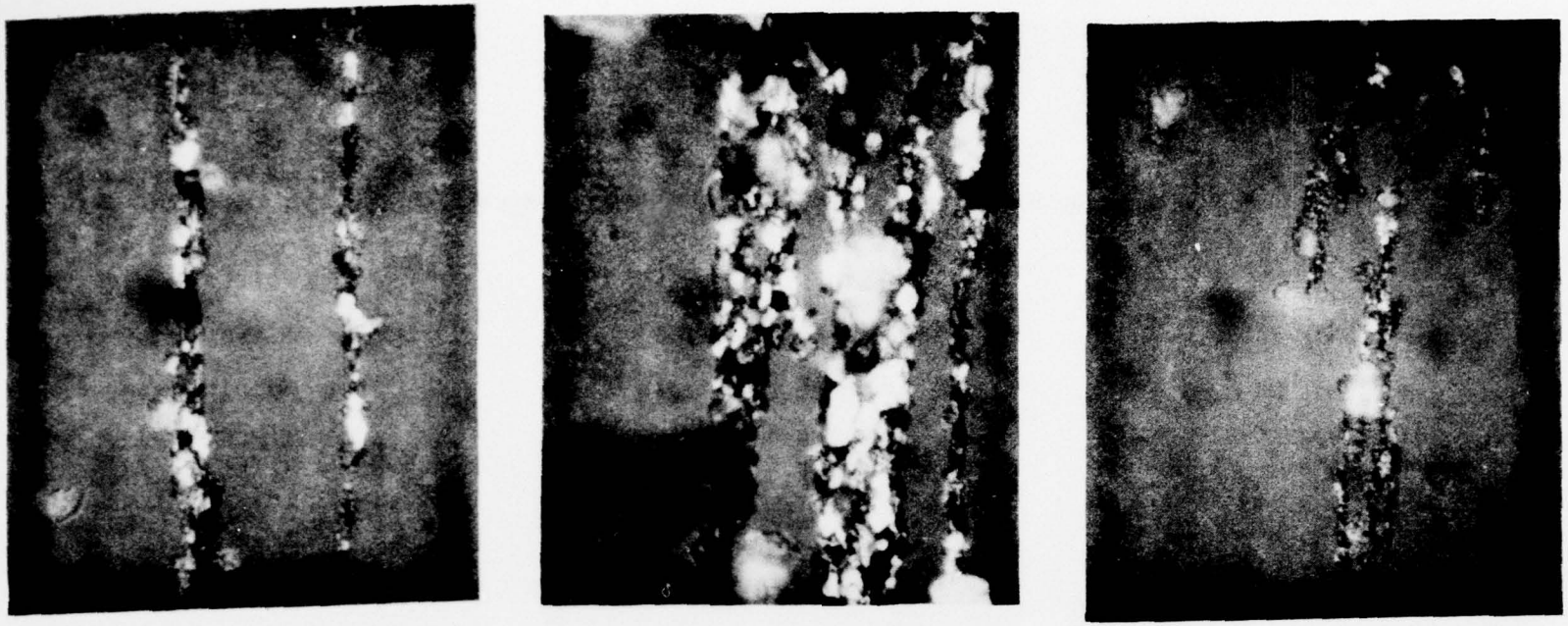

(a)
AFTER EXPOSURE TO
0-5 μM PARTICLE
SIZE RANGE

(b)
AFTER EXPOSURE TO
0-30 μM PARTICLE
SIZE RANGE

(c)
AFTER EXPOSURE TO
0-80 μM PARTICLE
SIZE RANGE

Fig. 57. Ferrograms of Wear Debris (54mm) from Linear Mechanism (Cast Iron–Steel) after Exposure to 5 mg/litre of Contaminant (Magnification = 1000).

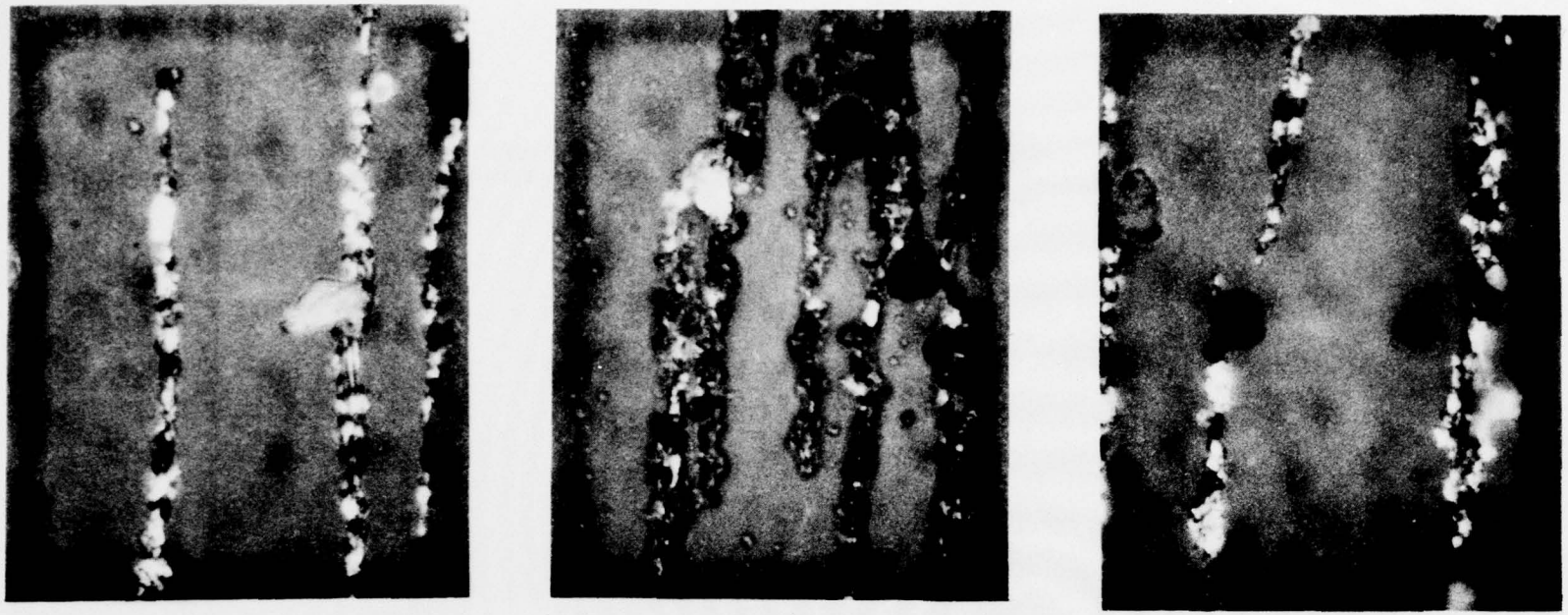

(a)
AFTER EXPOSURE TO
0-5 μM PARTICLE
SIZE RANGE

(b)
AFTER EXPOSURE TO
0-30 μM PARTICLE
SIZE RANGE

(c)
AFTER EXPOSURE TO
0-80 μM PARTICLE
SIZE RANGE

Fig. 58. Ferrograms of Wear Debris (54mm) from Linear Mechanism (Cast Iron–Steel) after Exposure to 10 mg/litre of Contaminant (Magnification = 1000).

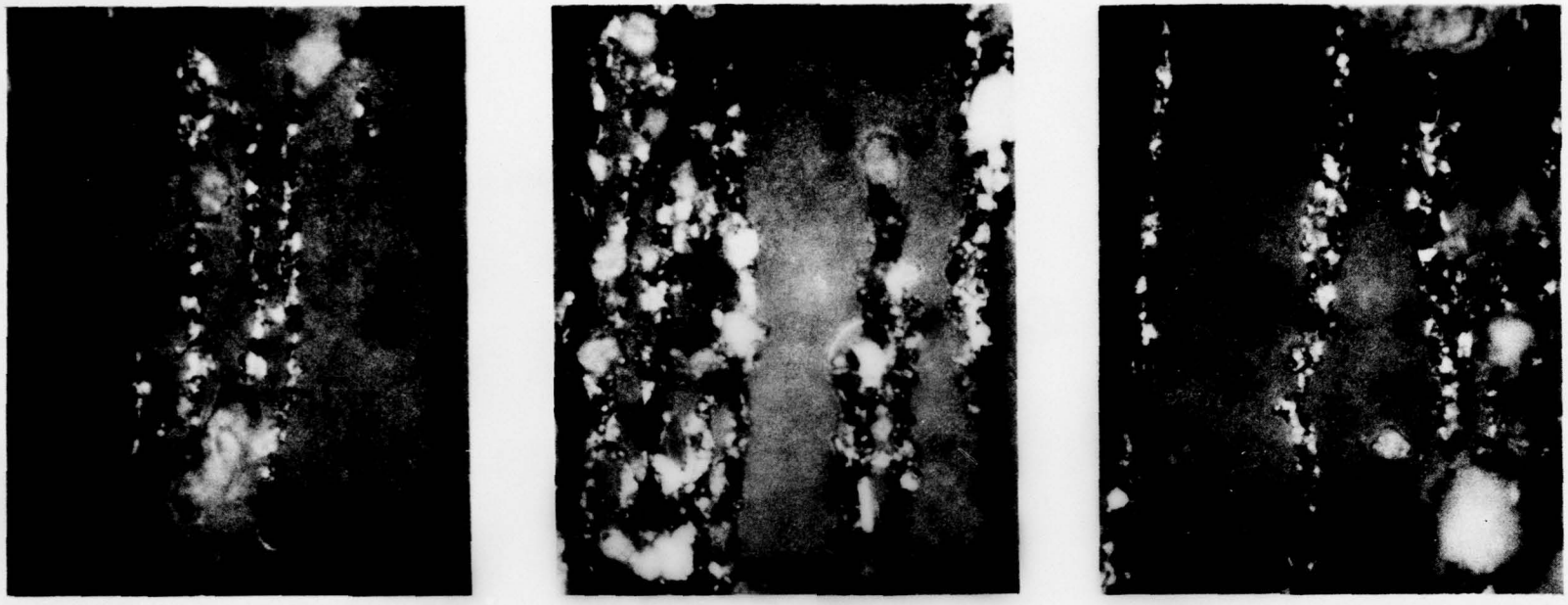

(a)
AFTER EXPOSURE TO
0-5 μM PARTICLE
SIZE RANGE

(b)
AFTER EXPOSURE TO
0-30 μM PARTICLE
SIZE RANGE

(c)
AFTER EXPOSURE TO
0-80 μM PARTICLE
SIZE RANGE

Fig. 59. Ferrograms of Wear Debris (54mm) from Linear Mechanism (Cast Iron–Steel) after Exposure to 20 mg/litre of Contaminant (Magnification = 1000).

(a)
AFTER EXPOSURE TO
0-5 μM PARTICLE
SIZE RANGE

(b)
AFTER EXPOSURE TO
0-30 μM PARTICLE
SIZE RANGE

(c)
AFTER EXPOSURE TO
0-80 μM PARTICLE
SIZE RANGE

Fig. 60. Ferrograms of Wear Debris (54mm) from Linear Mechanism (Cast Iron–Steel) after Exposure to 40 mg/litre of Contaminant (Magnification = 1000).

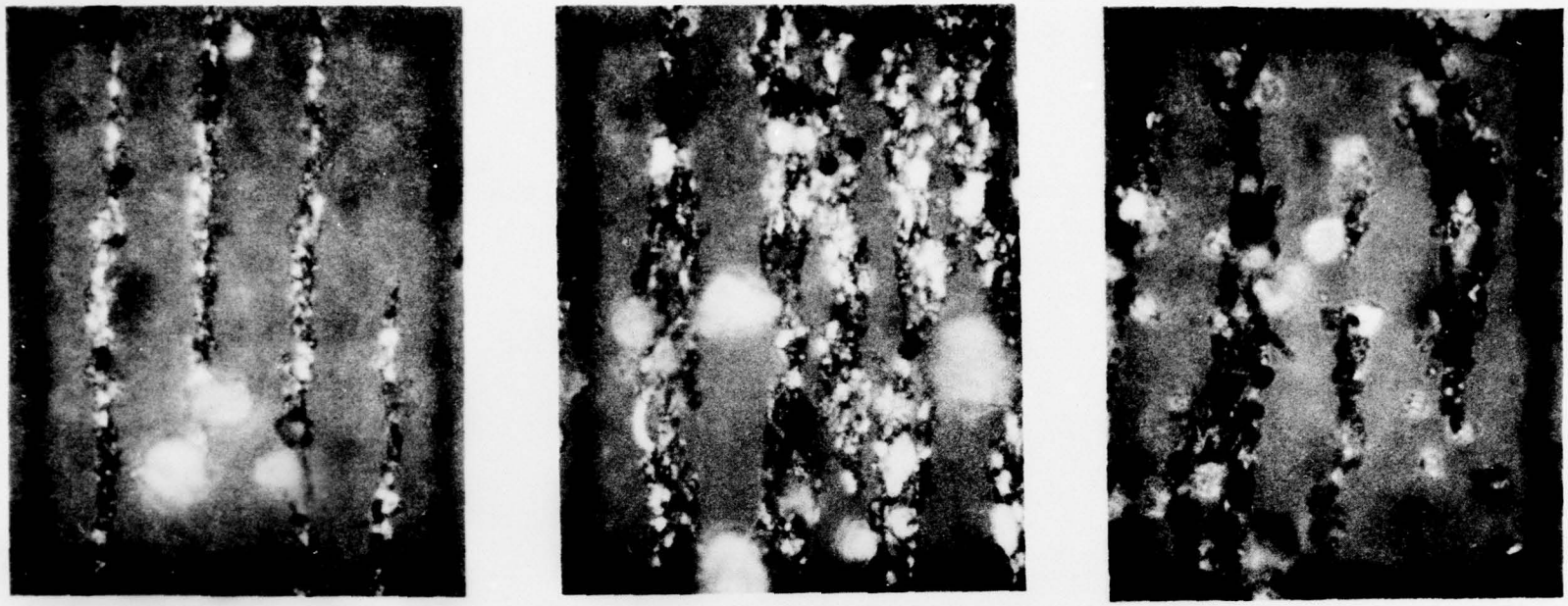

(a)
AFTER EXPOSURE TO
0-5 μM PARTICLE
SIZE RANGE

(b)
AFTER EXPOSURE TO
0-30 μM PARTICLE
SIZE RANGE

(c)
AFTER EXPOSURE TO
0-80 μM PARTICLE
SIZE RANGE

Fig. 61. Ferrograms of Wear Debris (54mm) from Linear Mechanism (Cast Iron–Steel) after Exposure to 80 mg/litre of Contaminant (Magnification = 1000X).

CHAPTER VIII

SUMMARY AND CONCLUSIONS

This report covers the activities of the first year of a program whose primary goal is the investigation of life improvements of hydraulic components brought about by the removal of particulate contamination entrained in the fluid of hydraulic systems. There is no doubt that contaminant wear in fluid power components is a critical factor which influences the life and reliability of hydraulic systems. The most logical answer to the problem of reducing contaminant wear and improving component life is to remove the entrained contaminant. Such removal is accomplished by the addition to the system of a filter.

The contamination level in a hydraulic system must be considered on a dynamic basis. That is, contaminant particles are continually ingested into the system fluid through ingression and generation, and the filter is continually removing such particles. A filter, by nature, is a proportional device in that it removes a given percentage of contaminant presented to it. Thus, the higher the system contamination level is, the more contaminant a given filter will remove. Therefore, the contamination level of a hydraulic system will stabilize at a value which forces the filter to remove the same amount of contamination that enters the system. It follows, then, that a more efficient filter will produce a lower contamination level in the system than a less efficient one.

The decision to incorporate a highly efficient filter into a hydraulic system requires some consideration. Generally speaking, a more efficient filter as compared to a less efficient filter will exhibit less contaminant capacity and a larger pressure drop. A reduced contaminant capacity will result in a shorter filter change interval, and a greater pressure drop will produce increased horsepower losses. In addition, the more efficient filter will usually have a higher initial cost. Thus, it should be obvious that there is added cost

involved in removing more of the contaminant. However, if the improvement in life and reliability of the system components is sufficient, this added cost can be offset. Therefore, the ultimate objective of this program is to determine the factors involved in life improvement through filtration of the system filter.

Since the number of factors involved in the study of contaminant wear of entire hydraulic components would become unmanageable, the approach taken here is first to investigate critical wear mechanisms of hydraulic components. The information derived through the study of such mechanisms could then be extrapolated to the component. Two such mechanisms were selected. A rotary device incorporating a stationary disk and a rotating disk are used to simulate one of the crucial hydraulic wear mechanisms, and a linear reciprocating device is used to simulate another. Each of these mechanisms was subjected to various particle size ranges and concentration of a test contaminant produced from AC Fine Test Dust stock. The results reported here are for a given surface clearance and a designated operating condition for the devices.

In extrapolating the results of the tests to hydraulic components, it must be kept in mind that the surface clearances were maintained at a constant value. Such constant clearance is not representative of a hydraulic component over its entire life but is sufficient to discuss the contaminant wear in some interval of life. As data are produced at other clearances, the characteristics of the components over their whole life will become lucid. (These tests will be run during the next year.)

The results of the rotary mechanism tests indicate that, at higher concentration, the particle size distribution is very critical. The relation between particle size range and wear as revealed by the wear debris density becomes non-linear at concentrations greater than 80 mg/litre. This means that, if a system contains 80 mg/litre of contaminant, more life improvement will be gained in reducing the particle size distribution from 0-30 micrometres to 0-5 micrometres than will be gained by going from 0-80 micrometres to 0-30 micrometres.

This is true for both the brass/steel and the aluminum/steel combinations. Reducing the contaminant concentration decreases the amount of wear produced by the contaminant at all particle sizes with the rotary mechanism.

The data obtained during the testing of the linear mechanism revealed a considerably different wear characteristic than the rotary device. The 0-30 micrometres particle size range exhibited significantly more wear than either the 0-5 micrometres or 0-80 micrometres. These results are consistent with performance tests which have shown that the force to move such a mechanism will exhibit a maximum at some critical particle size distribution which is related to the clearance. This implies that reducing the particle size range (at a given concentration) of the entrained contaminant to which this type of device is subjected may not decrease the wear. To the project staff's knowledge, this is the first time that such data have been obtained for reciprocating elements.

Experience with hydraulic systems has revealed that, in most cases, the pump is the most sensitive component to the attack of contaminant. The two mechanisms utilized in this program are representative of the wear mechanisms found in the majority of hydraulic pump designs. In addition, the linear device also simulates the critical wear surfaces found in hydraulic valves. Therefore, the results of these tests can be reasonably projected to a hydraulic system (realizing the parametric constraints of the effort).

In general, if a system filter is replaced by a more efficient element to reduce contaminant wear, both the particle size distribution and the contaminant concentration will be decreased. Therefore, by assuming a change in contaminant level which might be achieved through a filter retrofit, some general statements concerning component life improvements can be formulated. Consider the three following hypothetical filter elements, which could be used to protect critical hydraulic components: Filter 1 products a contamination level of 80 mg/litre with a particle size distribution of 0-80 micrometres; Filter 2 achieves a level of 40 mg/litre and a distribution of 0-30 micrometres; while, Filter 3 is capable of stabilizing the system contamination level at 10 mg/litre of 0-5 micrometres. The contamination levels

produced by these hypothetical filters are depicted in Fig. 62. From the results of the tests presented in this report, hydraulic systems which incorporate three different types of wear mechanisms can be evaluated – rotary using brass/steel material, rotary using aluminum/steel, and a linear motion device.

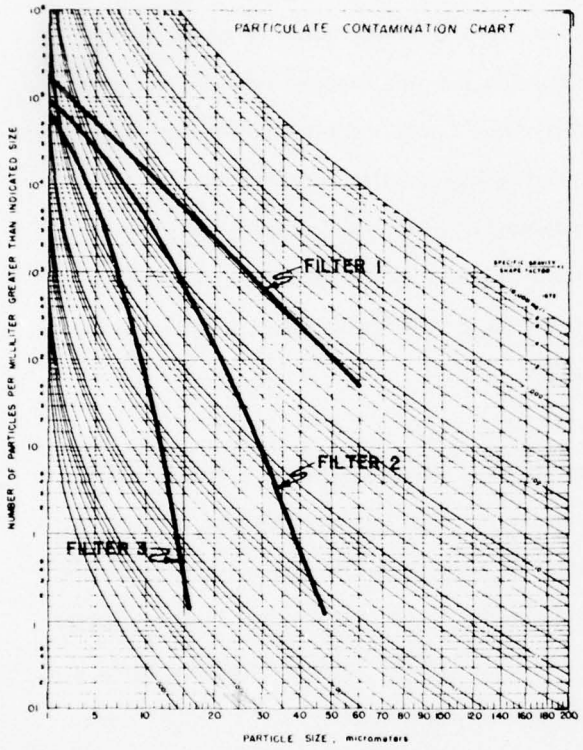

Fig. 62. Contamination Levels Produced By Hypothetical Filters 1, 2, and 3.

In a system where the primary wear process can be characterized by rotary motion with one brass and one steel surface, the test data reveal that changing from Filter 1 to Filter 2 would reduce the wear by 133% or could improve life by the same amount. This number can be found from Fig. 25 by subtracting the wear debris density at 40 mg/litre, 0-30 micrometres, which is about 4.2 from the density at 80 mg/litre, and 0-80 micrometres (9.8). Table 5 summarizes this type of information for the three mechanisms tested. The data for the rotary (aluminum/steel) tests can be found in Fig. 26, while the results of the linear mechanism tests are presented in Fig. 51. In addition, Fig. 63 graphically illustrates the wear reduction in the various mechanisms produced by the three hypothetical filters. In this figure, the number of particles per millilitre greater than the ten micrometres obtained from Fig. 62 is used to identify the contamination levels achieved by the three filters. This contamination level is plotted against wear as measured by Ferrographic densities to show the influence of each filter on the wear of the mechanisms.

TABLE 5. Summary of Wear Debris from Wear Mechanisms with Hypothetical Filters.

Description of Critical Mechanism	Wear Debris Density Obtained From Test		
	Filter 1 80mg/ℓ, 0.80	Filter 2 40mg/ℓ, 0.30	Filter 3 10mg/ℓ, 0.5
Rotary (brass/steel)	9.8	4.2	1.0
Rotary (aluminum/steel)	8.5	3.5	0.9
Linear (cast iron/steel)	6.3	6.3	1.8

TABLE 6. Summary of Life Improvement Estimates for Hypothetical Filters.

Filter Retrofit Plan		Estimated Life Improvement Percent		
		Mechanism Description		
From	To	Rotary Brass/Steel	Rotary Aluminum/ Steel	Linear
1	2	133	143	0
2	3	420	239	250
1	3	980	844	250

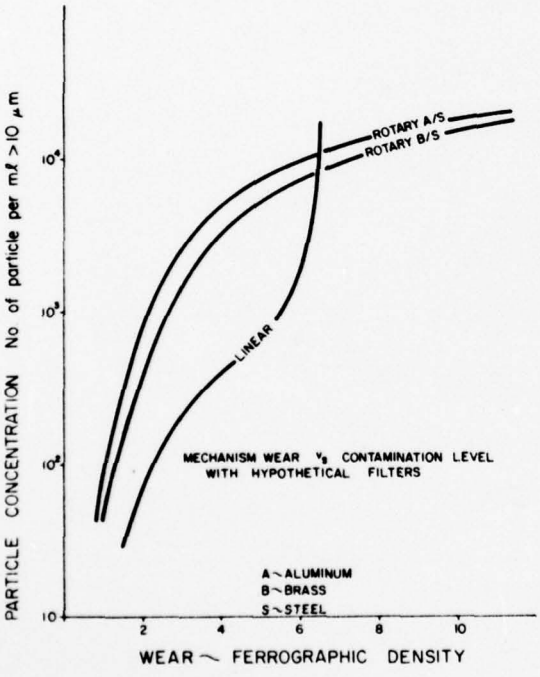

Fig. 63. Particle Concentration Produced by Hypothetical Filters versus Mechanisms Wear.

Table 6 summarizes the life improvement estimates for various filter wear mechanisms used for these tests. It cannot be emphasized enough that these estimates are based upon tests at only one clearance and one set of operating conditions, and they should be used with caution. As the test program proceeds and more data are obtained, these estimates can be and will be reconsidered. In addition, the hypothetical filters used in obtaining these estimates are just that – hypothetical. No attempt has been made to incorporate actual filter data nor to include a rigorous analysis of system ingression characteristics. It is felt that mechanism clearance, operating conditions, ingression characteristics, and actual filter performance could alter the estimates. However, based upon past

experience of the project staff, it is felt that the trend of life improvement is correct and the estimates substantiated by the test results.

REFERENCES

1. Bensch, L. E., and E. C. Fitch, *"A New Theory for the Contaminant Sensitivity of Fluid Power Pumps,"* Paper No. 72-CC-6, Fluid Power Research Center, Stillwater, Oklahoma, 1972.

2. *"Survey of Wear Processes and the Particles from Wear by Means of a Ferrograph,"* Final Report, October 1972. Prepared by Trans-Sonics, Inc., Burlington, Massachusetts, for the Office of Naval Research, Arlington, Virginia, under Contract No. N00014-72-C-0278, NR 229-005.

3. Finkin, E. F., *"Abrasive Wear,"* Special Technical Publication 446, American Society for Testing and Materials, 1916 Race Street, Philadelphia, Pennsylvania, 1969.

4. Khruschov, M. M., and M. A. Babichev, *"Resistance to Abrasive Wear of Structurally Inhomogenous Materials,"* **Friction and Wear in Machinery**, Vol. 12, Translated from Russian, American Society of Mechanical Engineers, 1960, pp. 5-24.

5. Spurr, R. T., and T. P. Newcomb, *"The Friction and Wear of Materials Sliding Against Unlubricated Surfaces of Different Types and Degrees of Roughness,"* **Proceedings of the Conference on Lubrication and Wear**, Institution of Mechanical Engineers, London, England, 1957, pp. 269-275.

6. Avient, B.W.E., J. Goddard, and H. Wilman, *"An Experimental Study of Friction and Wear During Abrasion of Metals,"* **Proceedings**, Royal Society, Vol. 258A, London, England, 1960, pp. 159-180.

7. Toporov, G. V., *"The Influence of Structure on the Abrasive Wear of Cast Iron,"* **Friction and Wear in Machinery**, ASME Translation, Vol. 12, 1960, pp. 39-50.

8. Rabinowicz, E., L. A. Dunn, and P. G. Russell, *"The Abrasive Wear Resistance of Some Bearing Steels,"* **Journal of the American Society of Lubrication Engineers**, December 1961, pp. 587-593.

9. Nathan, G. K., and W.J.D. Jones, *"Influence of the Hardness of Abrasives on the Abrasive Wear of Metals,"* **Proceedings**, Institute of Mechanical Engineers, Vol. 181, Part 30, London, England, 1966-67, pp. 215-221.

10. Khruschov, M. M., *"Resistance of Metals of Wear By Abrasion as Related to Hardness,"* **Proceedings of the Conference on Lubrication and Wear**, Institution of Mechanical Engineers, London, England, 1957, pp. 655-659.

11. Bitter, J.G.A., *"A Study of Erosion Phenomena, Part I,"* **Wear**, Vol. 6, 1963, pp. 5-21.

12. Bitter, J.G.A., *"A Study of Erosion Phenomena, Part II,"* **Wear**, Vol. 6, 1963, pp. 169-190.

13. Fitch, E. C., *"Component Contaminant Sensitivity – A Status Report on Pumps,"* **Proceedings of the National Conference on Fluid Power**, Vol. XXVII, Philadelphia, Pennsylvania, 1974.

14. Fitch, E. C., *"Measuring Contaminant Tolerance in Terms Compatible with Filtration Specifications – New Research Findings,"* Symposium on Contamination Control to Benefit Man and Product, Svenska Massan, Gothenburg, Sweden, April 1975.

15. Fitch, E. C., and R. K. Tessmann, *"Controlling Contaminant Wear Through Filtration,"* Third International Tribology Conference (Tribology for the Eighties), Aberdeen, Scotland, Paisley College of Technology, September 1975.

16. Scott, D., W. W. Seifert, and V. C. Westcott, *"The Particles of Wear,"* **Scientific American**, Vol. 230, No. 5, May 1974, pp. 88-97.

17. American National Standard Association, *"American National Standard Method for Calibration of Liquid Automatic Particle Counters Using AC Fine Test Dust, ANSI B93.28-1973,"* New York, NY, 1973.

18. Seifert, W. W., and V. C. Westcott, *"A Method for the Study of Wear Particles in Lubricating Oil,"* **Wear**, Vol. 21, No. 1, August 1972.

19. Seifert, W. W., and V. C. Westcott, *"Investigation of the Iron Content of Lubricating Oil Using Ferrograph and Emission Spectrometer,"* **Wear**, Vol. 23, No. 2, 1973.

20. Westcott, V. C., *"Predicting and Determining Failures by Means of Ferrography,"* Ninth Annual FAA International Maintenance Symposium, Washington, D. C., December 11-13, 1973.